Nation Cheng Kung University

Institute of Space and Plasma Sciences

110 Annual Reprot

研究生：郭名翔 Ming-Hsiang Kuo

指導教授：張博宇 Po-Yu Chang

Abstract

In our study, the plasma jet can be generated from the laboratory and will be used to simulate astrophysical objects. The plasma jet was generated by the conical-wire array. Conical-wire arrays are used four tungsten wires with a diameter of 20 μm. The conical-wire array was driven by the pulsed-power system. The pulsed-power system provides a pulsed current with a peak of ∼135 kA and a rise time of ∼1.6 μs. The velocity of the plasma jet can be measured by the Jet-velocity measurement system. The velocity of the plasma jet generated by the conical-wire array was ∼90 km/s. Further, we studied the angular momentum of the rotating plasma jet. The rotating plasma jet was generated by the twisted-conical-wire array. Furthermore, we want to study the evolution of the plasma disk that is generated from two plasma jets colliding with each other. Therefore, we design the bi-conical-wire array generating the counter-propagate plasma jets to generate plasma disk. For plasma measurements, we have visible-light camera system and laser camera system. The visible-light camera system viewing from the side was already built by the former student Yen-Cheng Lin. Therefore, I built the one viewing from the top. On the other hand, the laser camera system using the Q-switch laser with a pulse width of ∼ 5 ns in 532 nm to capture the schlieren and shadowgraph images. Finally, to keep the optical components clean and air cooling for the laser, we built the Fan Filter Unit (FFU) for the optical table. The lighting for the optical table using the Light-Emitting Diode (LED) light strip was also built.

Contents

1 The plasma jet **8**

1.1 The conical-wire array . . . 9

1.2 The jet-velocity measurement . . . 9

1.2.1 The lens testing experiment . . . 11

1.2.2 The LensHolder . . . 12

1.2.3 The FiberHolder . . . 13

1.2.4 The AlignmentStand . . . 14

1.2.5 Jet-velocity measurement result . . . 15

1.2.6 Summary . . . 16

1.3 The rotating plasma jet . . . 16

1.4 The bi-conical-wire array . . . 17

1.4.1 Experimental result . . . 19

2 Top-View camera **21**

2.1 Summary . . . 23

3 The optical table system **24**

3.1 The Fan-Filter Unit (FFU) . . . 24

3.2 The Light-Emitting Diode (LED) light strip . . . 25

4 Future work **26**

5 Summary **28**

References **29**

A Appendix **30**

A.1 The CAD drawing of the LensHolder . . . 30

A.2 The CAD drawing of the HolderSupport . . . 35

A.3 The CAD drawing of the FiberHolder . . . 40

A.4 The CAD drawing of the AlignmentStand . . . 44

A.5 The PowerBoard Layout for the AlignmentStand . . . 47

A.6 The CAD drawing of the bi-conical-wire array 48
A.7 The CAD drawing of the Top-view camera cage 56

List of Figures

1 The plasma jet visible light image.[1] 8

2 (a) The cross-section of conical-wire array. (b) The conical-wire array. 9

3 The schematic diagram of measurement system. 10

4 The jet-velocity measurement system. 10

5 The jet-velocity meansurement system and subsystem. 11

6 (a) The camera lens Nikon AF NIKKOR 70-300mm. (b) The experiment setup 12

7 (a) The LensHolder. (b) The cross section of RingHolder. 13

8 (a) The FiberHolder. (b) The set of M3 attachment. 13

9 (a) The FiberSupport. (b) The fiber core and tube. (c) The set of fiber attachment. 14

10 (a) The AlignmentStand. (b) The lighted AlignmentStand. (c) The image of AlignmentStand. 15

11 The data of Experiment NO 20210816. 16

12 (a) The twisted-conical-wire array. (b) Shadowgraph image of rotating plasma jet. (c) Top view of rotating plasma jet. 17

13 (a) The schematic diagram of plasma disk. (b) The cross-section of the bi-conical-wire array. 18

14 The structure of the bi-conical-wire array. 18

15 (a) The bi-conical-wire array. (b) The actual bi-conical-wire array. 19

16 The experiment of bi-conical-wire array visible-light image 20

17 (a) The Schlieren image of the bi-conical-wire array (b) The Shadowgraph image of the bi-conical-wire array 20

18 (a) The top-view camera cage. (b) The actual top-view camera. (c) The structure of the top-view camera. 21

19 (a) The cross-section of the Base Plate and ISO100 flange. (b) The CAD drawing of the Base Plate. 22

20 (a) The cross-section of the Middle Plate and Base Plate. (b) The CAD drawing of the Middle Plate. 22

21 The cross-section of the Middle Plate and the Battery Plate. 23

22 The image captured from the top-view camera. 23

23 (a) The power switch and pilot lamp (b) The circuit diagram of FFU system . . 24
24 (a) The control panel (b) The LED light strips (c) The circuit diagram of the switch box 25
25 (a) The gray value profile of the lower tungsten wire. (b) The gray value profile of the upper tungsten wire. 26
26 The bi-conical-wire array with insulated middle layer and metal top disk. 27
27 (a) The image of experiment NO. 20211230. (b) The image of experiment NO. 20220217. (c) The image of experiment NO. 20220224. 27

List of Tables

1 The parameter of different focal length 11

2 The data of jet-velocity Measurement System 16

3 The different version of bi-conical-wire array. 27

1 The plasma jet

We are using the one-kilojoule pulsed-power generator to study astrophysics in the laboratory[1]. The plasma jet and the plasma disk will be used to simulate astrophysical objects. The plasma jet is generated by the conical-wire array driven by the pulsed-power system. Further, we used the twisted-conical-wire array to generate rotating plasma jet[2]. Furthermore, we want to study the conservation of angular momentum in a plasma disk. The plasma disk can be generated by a bi-conical-wire array. The twisted bi-conical-wire array generates two counter-propagating plasma jets colliding with each other creating the rotating/non-rotating plasma disk. We have a visible-light camera system to capture the time-integrated image from the side and from the top. On the other hand, the laser-camera system can capture time-resolved images for schlieren image and shadowgraph image from the side, respectively. Furthermore, we built a jet-velocity measurement system using a pair of photodiodes. The conical-wire array is described in section 1.1. The jet-velocity measurement system is described in section 1.2. The rotating plasma jet is described in section 1.3. In section1.4 will introduce the bi-conical-wire array.

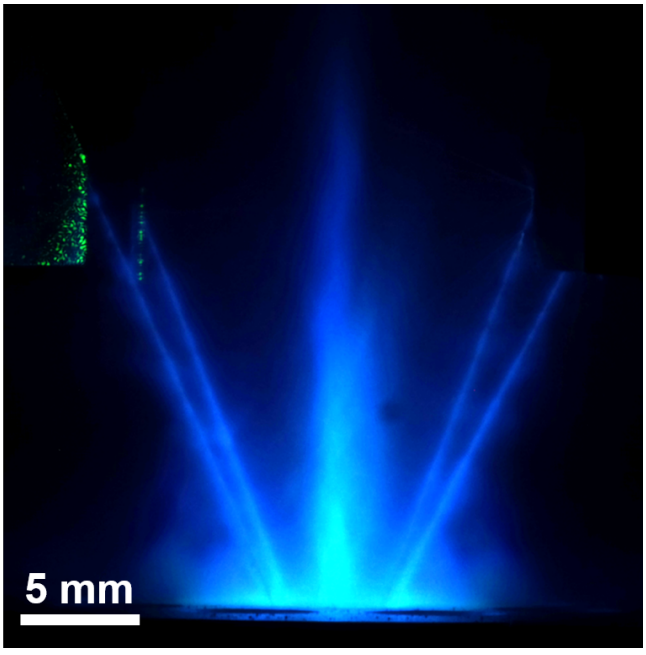

Figure 1: The plasma jet visible light image.[1]

1.1 The conical-wire array

The conical-wire array is used to generate the plasma jet. The conical-wire consistes of 4 tungsten wires with a diameter of 20 μm. Tungsten wires have 30° inclined to the z-axis. Figure 2(a) shows the cross-section of the conical-wire array. Figure 2(b) shows the actual conical-wire array. The conical-wire array is driven by the pulsed-power system. The pulsed-power system provides a pulsed current with a peak of ∼135 kA and a rise time of ∼1.6 μs[1]. When current passes through the tungsten wires, the coronal plasma is ablated from the tungsten wires and merge at the center of the conical-wire array through the z-pinch effect. In our research, the plasma jet velocity is ∼90 km/s, measured by the jet-velocity measurement system introduced in section 1.2.

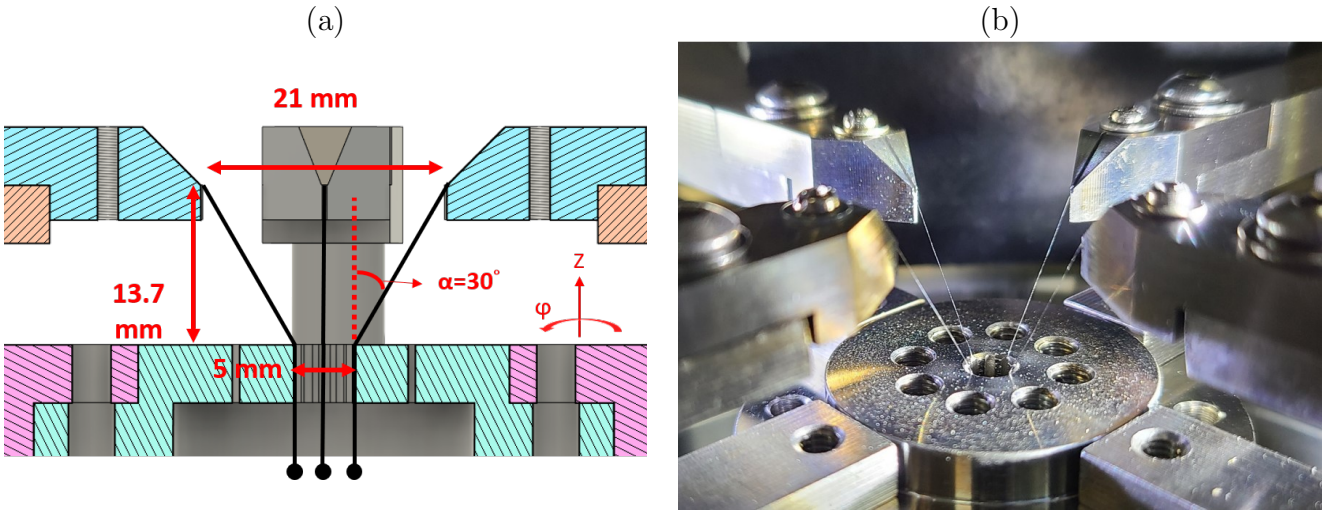

Figure 2: (a) The cross-section of conical-wire array. (b) The conical-wire array.

1.2 The jet-velocity measurement

We use two photodiodes at different locations to detect the plasma jet for measuring the jet velocity. The time difference of the photodiode signal can be used to calculate the velocity of the plasma jet. Figure 3 is the schematic diagram of the measurement system. There is a pair of fibers set on the imaging plane to detect the self-emission signal from the plasma jet reaching different locations on the object plane. Figure 4(a) shows the top-view of the jet-velocity measurement system. The fiber consists of a central core[3] with a numerical aperture of 0.5 and a cover tube[4], as shown in figure 4(b). Figure 5 shows the subsystems of the jet-velocity measurement system and the components of each subsystem. The system

consists of four subsystems: LensHolder, FiberHolder, AlignmentStand, and Photodiode. The plasma jet is in the vacuum chamber. However, we want to observe the plasma jet outside of the vacuum chamber. Therefore, the optical imaging system is used to achieve non-contact detection and free from Electromagnetic pulse (EMP). Further, the photodiodes of the system are the DET10A2 Si biased detector made by Thorlab[5]. The photodiode has a 1-ns rise time to detect the signal in the nanosecond scale. Furthermore, we need to study the magnification and the image distance of the imaging system. The study will be discussed in section 1.2.1. On the other hand, the LensHolder holds the camera lens and keeps it level. The LensHolder is described in section 1.2.2. Meanwhile, the FiberHolder holds the fiber at the imaging plane and it is described in section 1.2.3. To determine the fiber location, we designed the AlignmentStand. The AlignmentStand is described in section 1.2.4. The result of the jet-velocity measurement system will be presented in section 1.2.5. The plasma jet velocity was ~90 km/s measured by the jet-velocity measurement system.

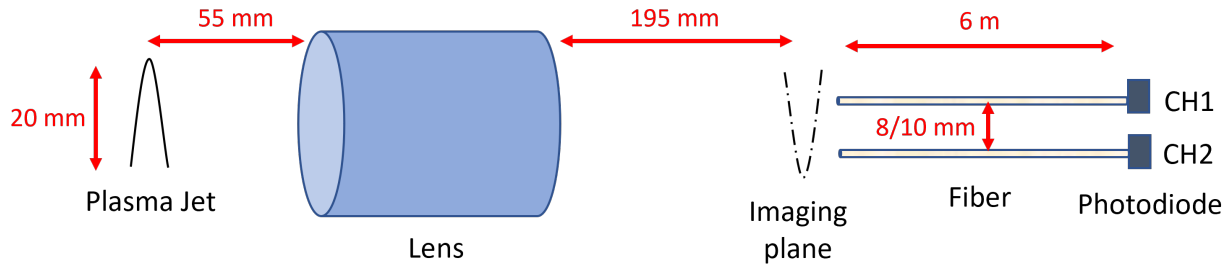

Figure 3: The schematic diagram of measurement system.

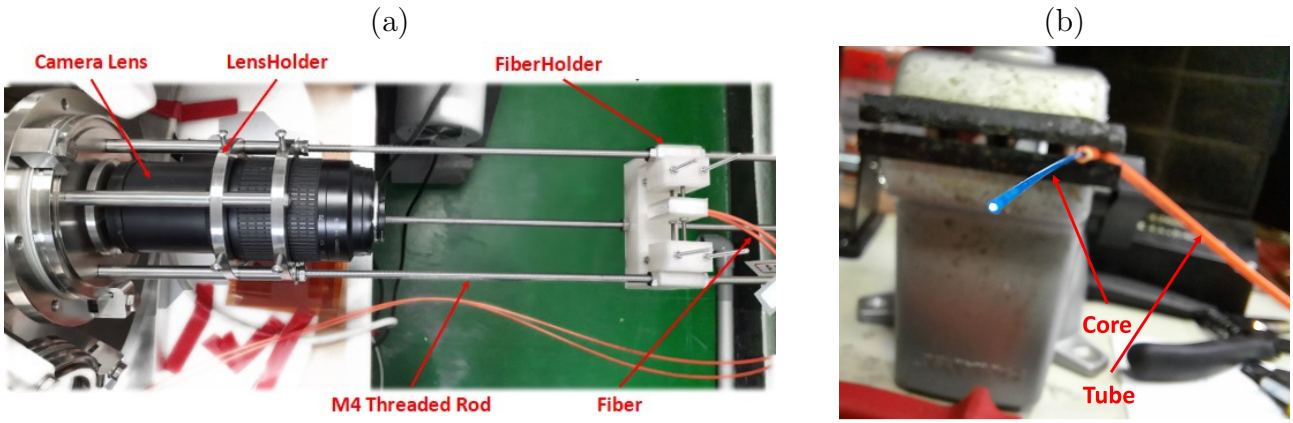

Figure 4: The jet-velocity measurement system.

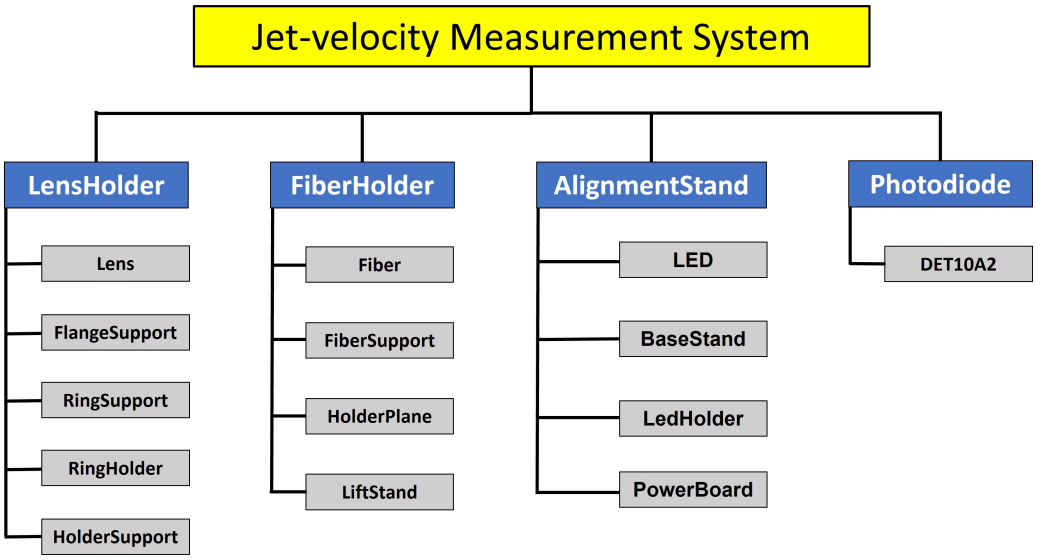

Figure 5: The jet-velocity meansurement system and subsystem.

1.2.1 The lens testing experiment

The camera lens we use is a zoom lens that has changeable focal lengths and magnifications. This experiment is to find the suitable image distance and the magnification. The camera lens is Nikon AF NIKKOR 70-300 mm and is shown in figure 6(a). Figure 6(b) is the experimental setup. A LED with a size of 4 mm is used to mimic the plasma jet. The object distance is 55 cm for simulating the plasma jet at the center of our vacuum chamber being viewed through the ISO 100 flange. Therefore, the distance between the LED and the lens is the fixed parameter. The focal length is the controlled variable in the experiment that affects the image distance and the magnification. Table 1 shows the image distance and the magnification. The focal length in the range of 135 mm to 200 mm is the appropriate parameter for measuring the plasma jet velocity. For focal length longer than 200 mm, the image distance is too long so that the system would not fit into our pulsed-power system. Finally, the focal length and the magnification of the camera lens is set at 195 mm and 1 in the jet-velocity measurement system, respectively.

Table 1: The parameter of different focal length

Focal Length (mm)	Image Distance (cm)	Magnification
70	7.5	0.2
100	9.5	0.25
135	11.5	0.4
195	19.5	1
200	30	1.375
300	>100	none

(a) (b)

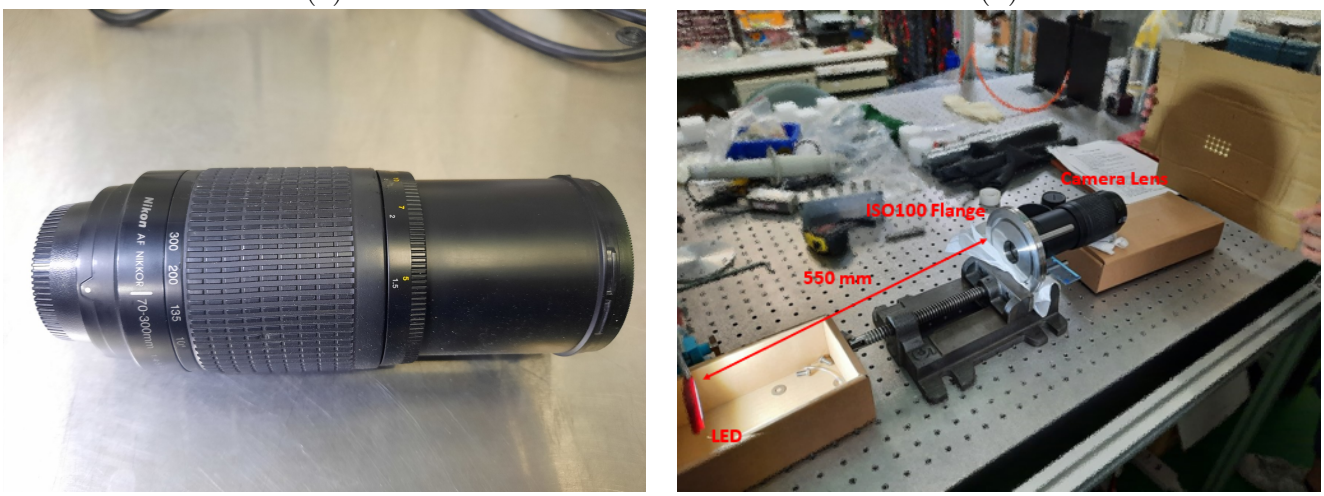

Figure 6: (a) The camera lens Nikon AF NIKKOR 70-300mm. (b) The experiment setup

1.2.2 The LensHolder

The LensHolder has a pair of RingHolders. The RingHolder is used to fix the camera lens and keep the camera lens level. The HolderSupport supports the LensHolder to ensure that the torque of the LensHolder's weight is not too large damaging the ISO100 flange. Figure 7(a) shows final assembly of the LensHolder. Figuer 7(b) is the cross section of the RingHolder. There are four through holes tapped with M4 thread from the side of the RingHolder. Thus, the camera lens is fixed by M4 screws. The FlangeSupports are screwed into the ISO100 flange and are connected with the 1st RingHolder. The 2nd RingHolder is connected with the 1st RingHolder through the RingSupport. Finally, two RingHolders are set on the HolderSupport. See Appendix A.1 and A.2 for CAD drawings.

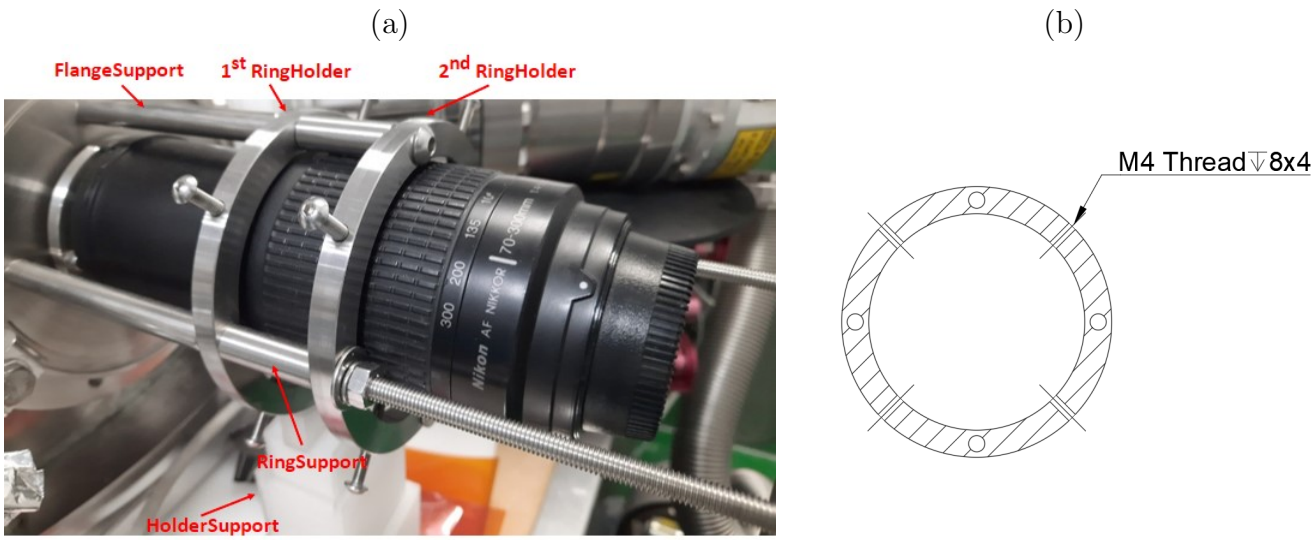

Figure 7: (a) The LensHolder. (b) The cross section of RingHolder.

1.2.3 The FiberHolder

Figure 8(a) shows the final assembly of the FiberHolder. The FiberHolder consists of the HolderPlane, LiftStand, FiberSupport, M3 threaded rods and the springs. The position of the FiberHolder can be moved along the M4 threaded rods connected with LensHolder, as shown in figure 4(a). Therefore, we can move the FiberHolder to the imaging plane of the camera lens. The LiftStand is connected with the HolderPlane using the M3 threaded rods. The M3 threaded rod is secured to the HolderPlane using a set of nuts, washers, and lock washers, as shown in figure 8(b).

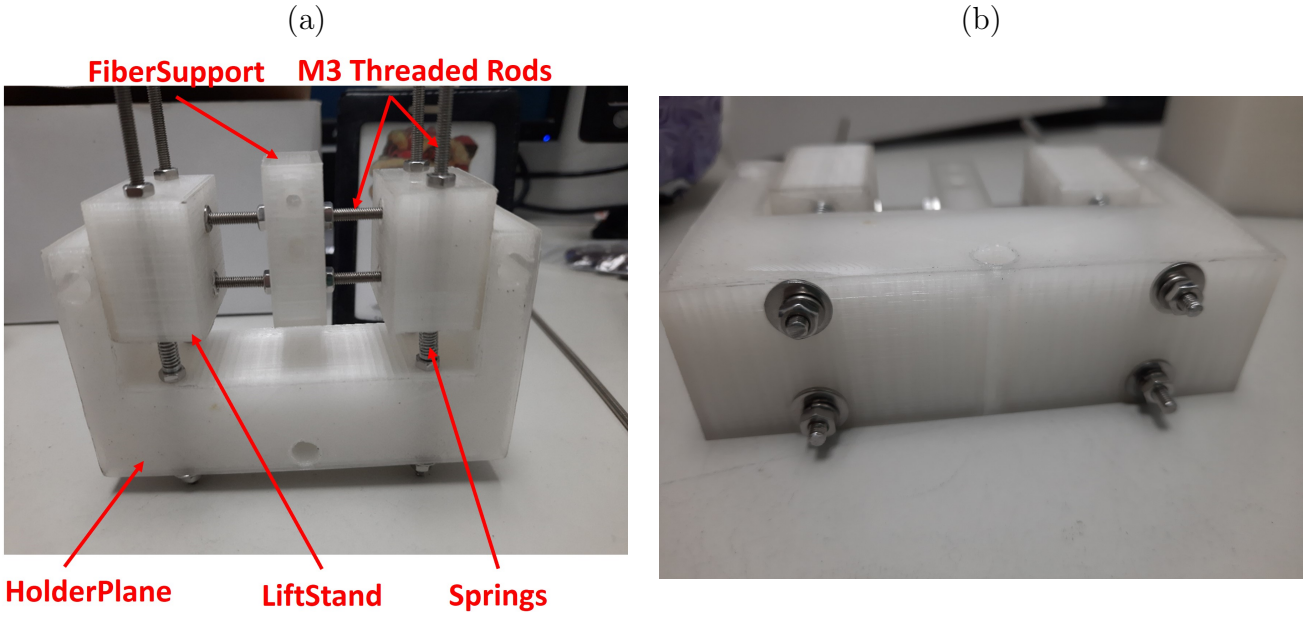

Figure 8: (a) The FiberHolder. (b) The set of M3 attachment.

Figure 9(a) shows the FiberSupport viewed from the chamber. The LiftStand uses a set of springs and nuts to move its position and thus adjust the FiberSupport's position in the Z direction. The FiberSupport is held on the M3 threaded rods and is free in the X direction. In other words, the position of the FiberSupport can be freely adjusted on the X-Z plane. The FiberSupport has a pair of holes to hold the fibers. The spacing of the pair of fiber holes is 8 mm. Figure 9(b) show the fiber core with the plastic nut and the plastic threaded rod. We drilled a hole in the plastic screw for the core to pass through. Next, we used cyanoacrylate adhesive to glue the fiber core to the plastic threaded rod. Afterward, the plastic nut locks on the plastic threaded rod to fix the fiber on the FiberSupport. Finally, the FiberHoler is moved to proper the position for the fiber to detect the plasma jet signal. See Appendix A.3 for CAD drawings.

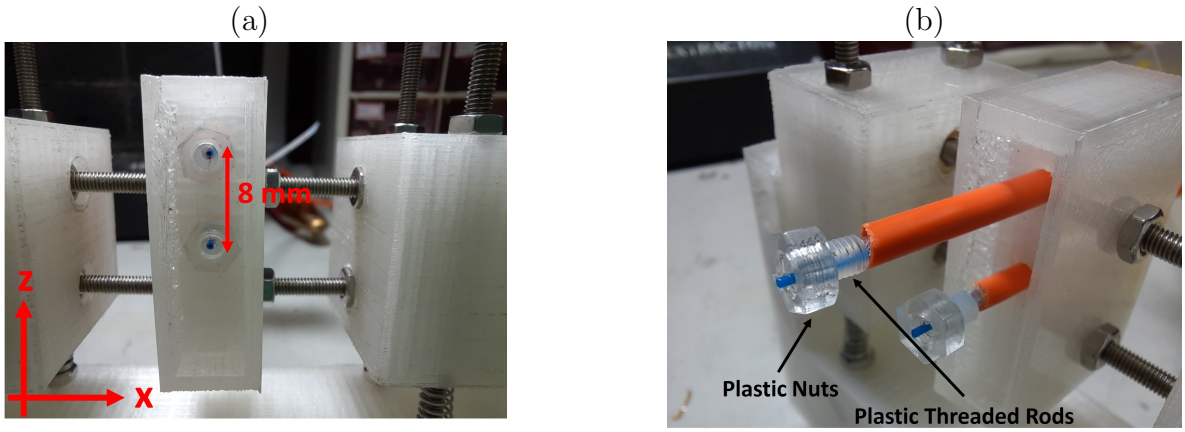

Figure 9: (a) The FiberSupport. (b) The fiber core and tube. (c) The set of fiber attachment.

1.2.4 The AlignmentStand

We use the AlignmentStand to determine the fiber position. The AlignmentStand acts as the pseudo target locates at where the plasma jet is generated in experiments. We will adjust the location of the fiber untill they are on the image plane. Figure 10(a) shows the AlignmentStand and the components of the light source. The battery powered LED lights up the AlignmentStand. The PowerBorad has a switch to control the battery output. See Appendix A.5 for the PowerBoard layout. The AlignmentStand is installed on the bottom of the conical-wire array, as shown in figure 10(b). The AlignmentStand is imaged on the FiberHolder by the camera lens, as shown in the red dashed box in figure 10(c). Therefore, we set the fiber position corresponding to the AlignmentStand image. In experiments, the fibers

sit on 5-mm and 13-mm above the bottom of the conical-wire array, respectively. See Appendix A.4 for CAD drawings.

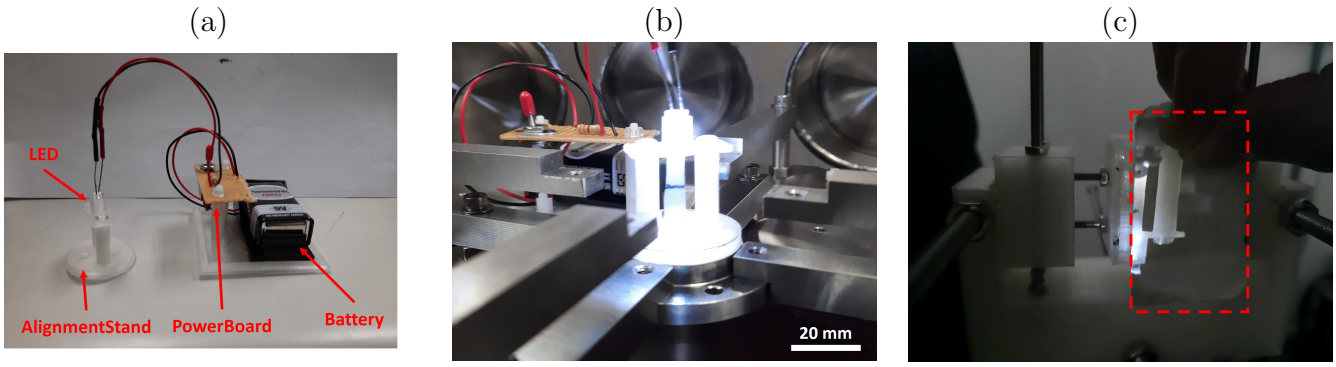

Figure 10: (a) The AlignmentStand. (b) The lighted AlignmentStand. (c) The image of AlignmentStand.

1.2.5 Jet-velocity measurement result

To measure the jet velocity, we use the oscilloscope to collect data from the photodiodes. Photodiode 1 and Photodiode 2 are set on the image of the plasma jet. Their locations are corresponding to 5 mm and 13 mm above the cathode, respectively. The signal increases when the image of the plasma jet passes through the photodiode. Afterward, we analyzed the data by the curve fitting. Figure 11 shows the data from two photodiodes in the experiment. We use Eq 1 as the fitting function to find the time of the foot of the data. Equation 1 is used to smooth the photodiode data and find the characteristics of the data. The red line in figure 11 is the fitted curve. The photodiode 1 signal occurs earlier than the photodiode 2 signal. On the other hand, the signal of Photodiode 1 is stronger than that of Photodiode 2. Because of the plasma is accumulated at the bottom and is ejected upward to form a jet. Table 2 shows the data from three different shots. Finally, the time difference and distance of the fiber can be used to calculate the plasma jet velocity. The calculate plasma-jet velocity is 90 $\pm$ 30.

$$F(t) = a\exp(b \times t) + c\exp(d \times t) \tag{1}$$

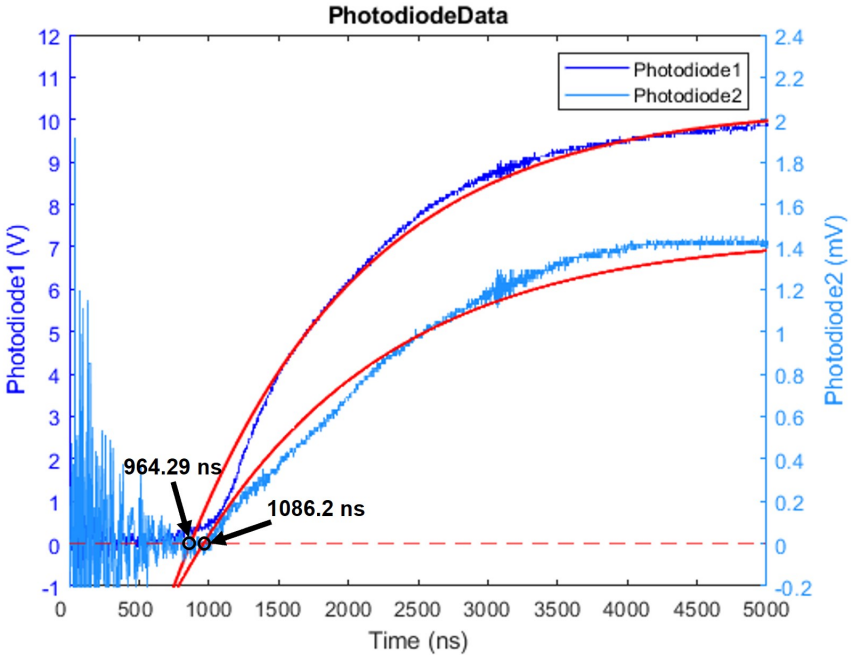

Figure 11: The data of Experiment NO 20210816.

Table 2: The data of jet-velocity Measurement System

Experiment NO	Photodiode 1 (ns)	Photodiode 2(ns)	Distance (mm)	Velocity (km/s)
20210812	818.61	962.56	8	55.57
20210813	925.25	991.48	8	120.79
20210816	964.29	1086.2	8	85.54
Mean ± SD				90 ± 30

1.2.6 Summary

In conclusion, we have built a system to measure to plasma-jet velocity. The plasma-jet velocity measured by the laser-camera system using the shadowgraph images and the schlieren images from the side was 170 ± 70[1]. As a result, the jet-velocity measurement system can measure the velocity of the high-speed plasma jet and can be used in other experiments in the future.

1.3 The rotating plasma jet

The rotating plasma jet was generated by a twisted-conical-wire array. Different from the conical-wire array introduced in section 1.1, the beams connecting wires to the anode are rotated. Therefore, the tungsten wires of the twisted-conical-wire array have rotating angle with respect to the cathode. Figure 12(a) shows the top view of the twisted-conical-wire array.

As a result, the coronal plasma with angular momentum is ablated from the tungsten wire using the twisted-conical-wire array. Finally, the rotating plasma jet splitted showing an upwardly rotating "tornado". Figure 12(b) shows the time-resolved shadowgraph image from the side of the rotating plasma jet. Figure 12(c) shows the time-integrated visible light image from the top of the rotating plasma jet. We observed the central hollow of the rotating plasma jet from the top-view time-integrated visible-light image. Therefore, the angular momentum conservation of the rotating plasma jet was observed from the side-view shadowgraph image and the top view visible-light image[6].

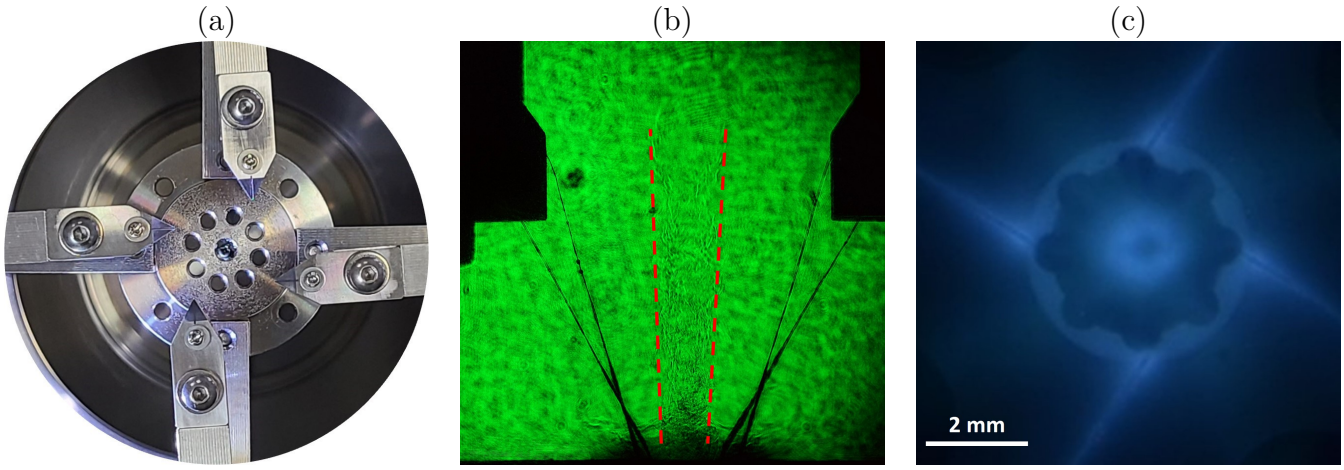

Figure 12: (a) The twisted-conical-wire array. (b) Shadowgraph image of rotating plasma jet. (c) Top view of rotating plasma jet.

1.4 The bi-conical-wire array

We want to study how the angular momentum evloves in the rotating/non-rotating plasma disk. The bi-conical-wire array is designed to generate two counter-propagating plasma jets colliding with each other to form the plasma disk. If the bi-conical-wire array is twisted, the plasma disk may rotate. Figure 13(a) shows the schematic diagram of how the plasma disk is generated.

Figure 13(b) shows the cross-section of the bi-conical-wire array. The bi-conical-wire array has the pair of head-on conical-wire array. The tungsten wires of the bi-conical-wire array also have a 30° inclination angle respect to the z-axis. Four tungsten wires with a diameter of 20 μm are used. The bi-conical-wire array has a three-layer structure. Figure 18 shows the enlarged structure of the bi-conical-wire array. See Appendix A.6 for the CAD drawing of the bi-conical-wire array. The upper conical-wire array is formed using the top layer and the

middle layer. The lower conical-wire array is formed using the middle layer and the bottom layer. The Middle Support is made of Polyoxymethylene to insulate the top and the middle layers. Therefore, current is forced to flow through tungsten wires. As a result, we use tungsten wires to connect the upper conical-wire array and the lower conical-wire array.

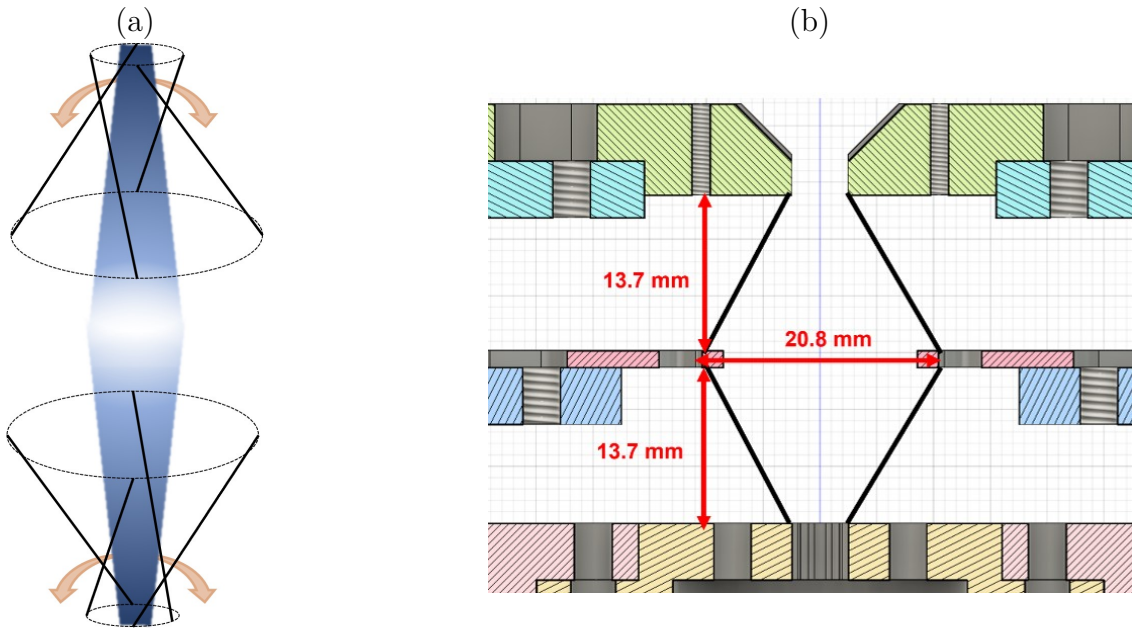

Figure 13: (a) The schematic diagram of plasma disk. (b) The cross-section of the bi-conical-wire array.

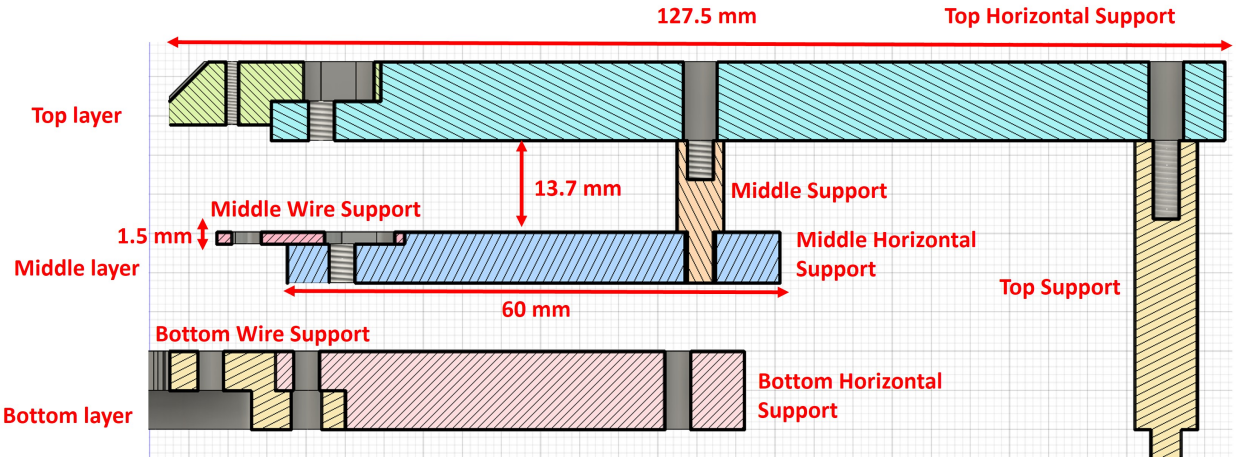

Figure 14: The structure of the bi-conical-wire array.

Figure 15(a) shows the CAD drawing of the bi-conical-wire array, where red arrows are the current paths. The pulsed current passes through the upper conical-wire array to the lower conical-wire array. Figure 15(b) shows the actual bi-conical-wire array and four tungsten wires. We expect that the bi-conical-wire array can generate plasma jets from both the upper conical-wire array and the lower conical-wire array.

(a) (b)

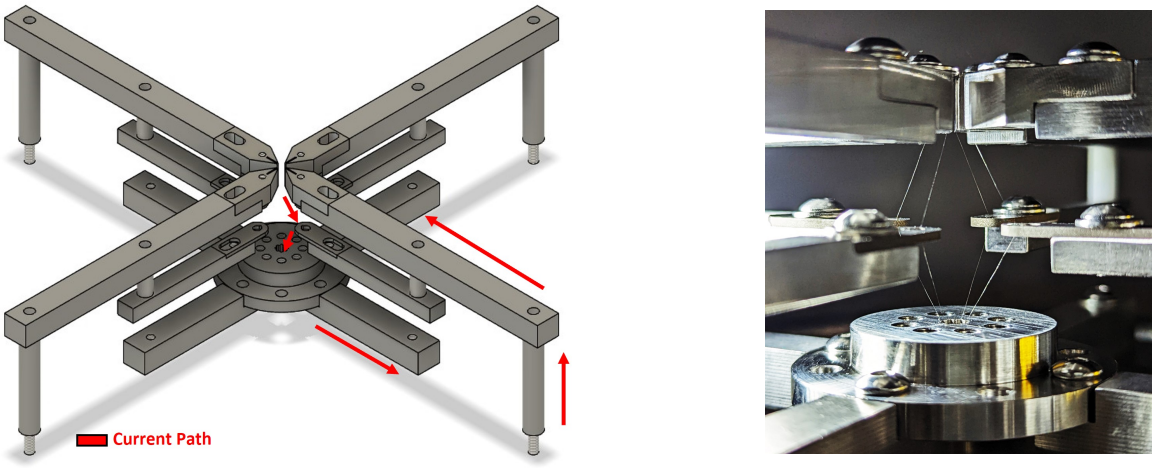

Figure 15: (a) The bi-conical-wire array. (b) The actual bi-conical-wire array.

1.4.1 Experimental result

In experiments, we captured time-integrated images using the visible-light camera system and time-resolved images using the laser-camera system. The laser camera system used the Q-switch laser with a pulse width of ~ 5 ns in 532 nm to capture the schlieren and shadowgraph images. The visible-light camera system captured the side-view and the top-view images. The top-view camera has an EMP-resisted cage to resist the electormagnetic noise. The top-view camera cage is described in Chapter 2. Figure 16 shows the visible-light image of the bi-conical-wire array. The time-integrated visible-light image from the side view shows the bi-conical-wire array has an asymmetric issue. The upper conical-wire array could not generate the plasma jet. Furthermore, images of the schlieren and shadowgraph in figure 17 also show that the upper conical-wire array could not accumulate enough plasma. Therefore, we need to resolve the asymmetric issue of the bi-conical-wire array. After the problem is solved, we will study the head-on collisions of two plasma jets.

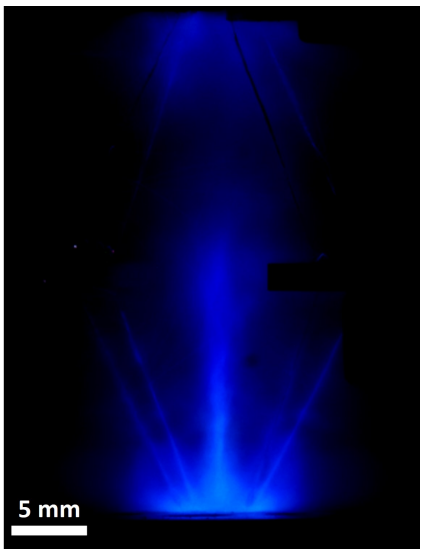

Figure 16: The experiment of bi-conical-wire array visible-light image

(a) (b)

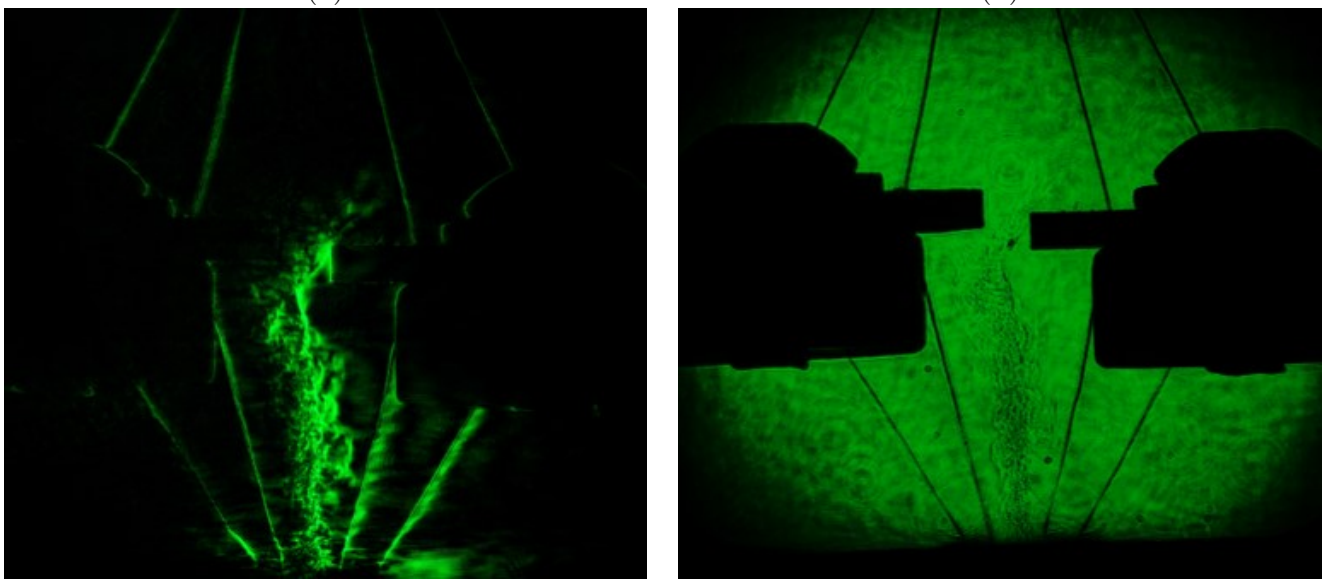

Figure 17: (a) The Schlieren image of the bi-conical-wire array (b) The Shadowgraph image of the bi-conical-wire array

2 Top-View camera

The top-view camera is used to capture the time-integrated visible-light image from the top. In our research, we use Raspberry Pi 4B[7] with the camera module[8] to capture images[2]. The camera was interfered by the EMP generated from the pulsed-power generator. For this reason, we use aluminum plates to form the Faraday cage to resist the EMP, as shown in figure 18(a). Figure 18(b) is the structure of the top-view camera. Figure 18(c) is the actual top-view camera. The top-view camera has a vertically developed structure and quick-release installation. See A.7 CAD drawing of the top-view camera cage.

(a) (b) (c)

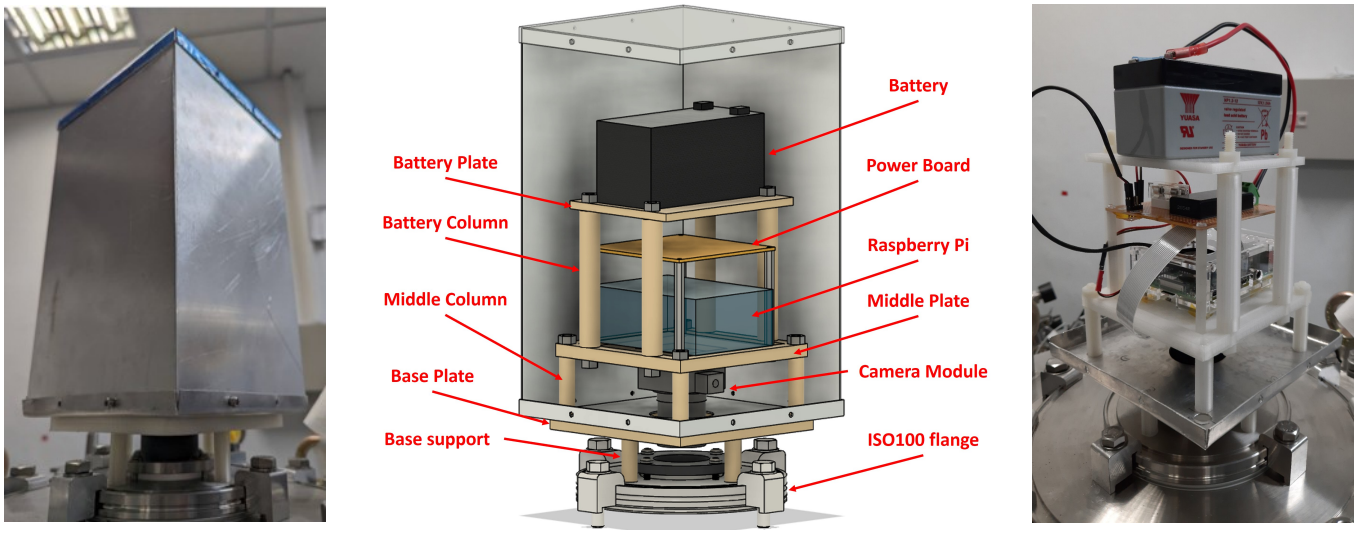

Figure 18: (a) The top-view camera cage. (b) The actual top-view camera. (c) The structure of the top-view camera.

The Base Plate of the top-view camera is fixed on the ISO100 flange to support its weight, as shown in figure19(a). For convenience, the components above the Base Plate can be quickly removed. The Base Pate has M6 counterbores and M6 recessed holes, as shown in figure 19. Therefore, the Base Plate can hide the screw heads and align the screws of the Middle Plate.

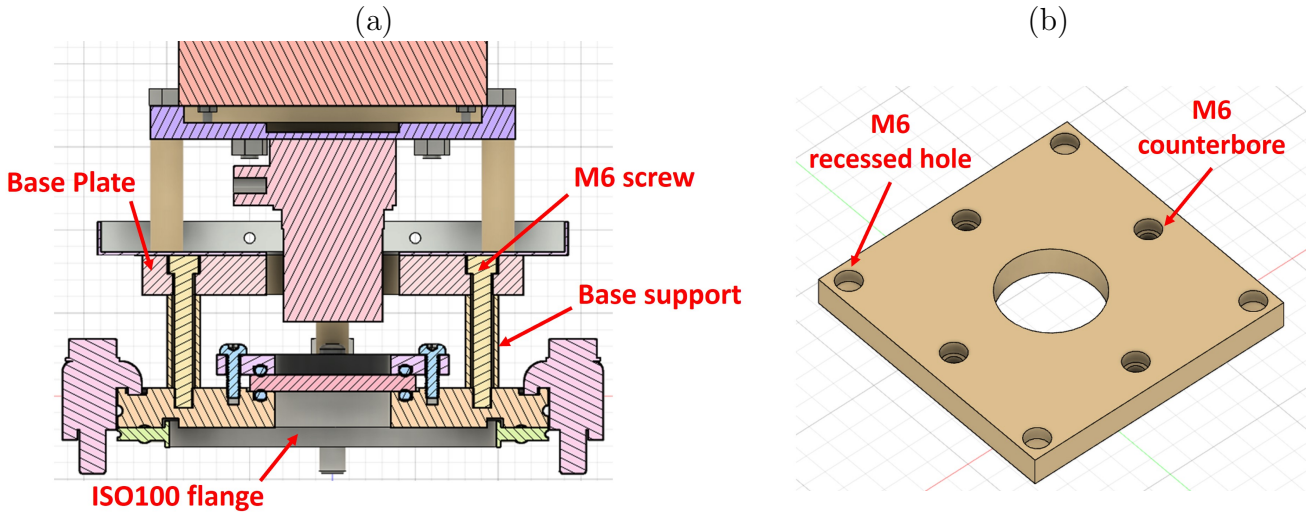

Figure 19: (a) The cross-section of the Base Plate and ISO100 flange. (b) The CAD drawing of the Base Plate.

Figure 20(a) shows the cross-section of the Middle plate and Base Plate. The Middle Plate uses M6 screws and M6 nuts to connect the Al Plate with the Middle Column. The M6 screw heads of the Middle Plate are inserted into M6 recessed holes of the Base Plate to stabilize the top-view camera. On the other hand, the Middle Plate connects with the camera module and the Power Board. The Raspberry Pi is put on the Middle Plate. Figure 20(b) shows the CAD drawing of the Middle Plate.

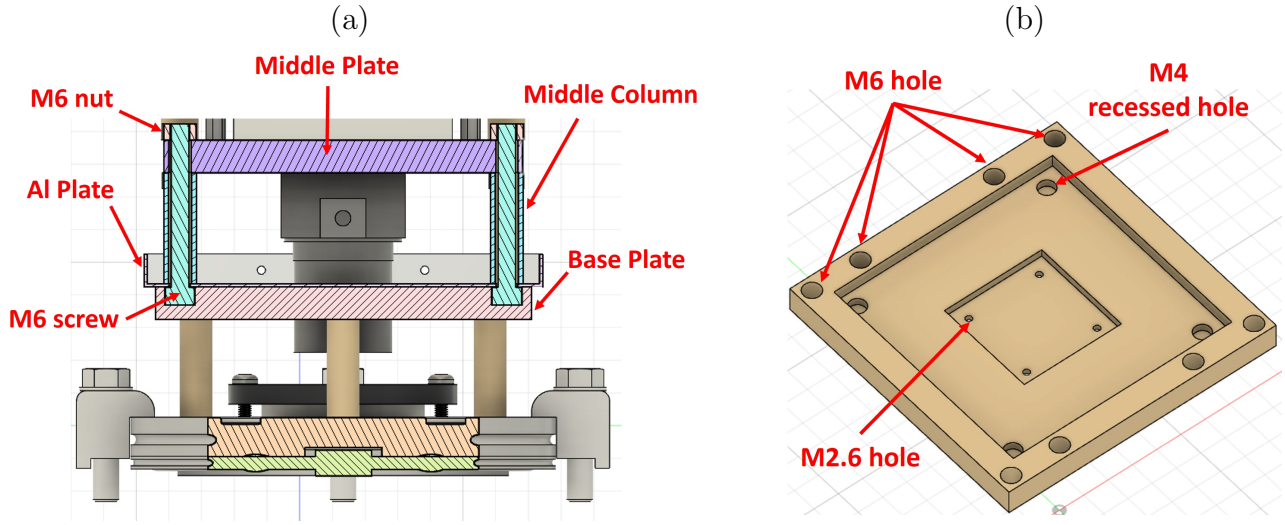

Figure 20: (a) The cross-section of the Middle Plate and Base Plate. (b) The CAD drawing of the Middle Plate.

Figure 21 shows the cross-section of the Middle Plate and the Battery Plate. The Battery Column has a pair of M6 recessed holes where M6 screws' heads are inserted. Therefore, the Battery Column connects the Middle Plate and supports the weight of the battery.

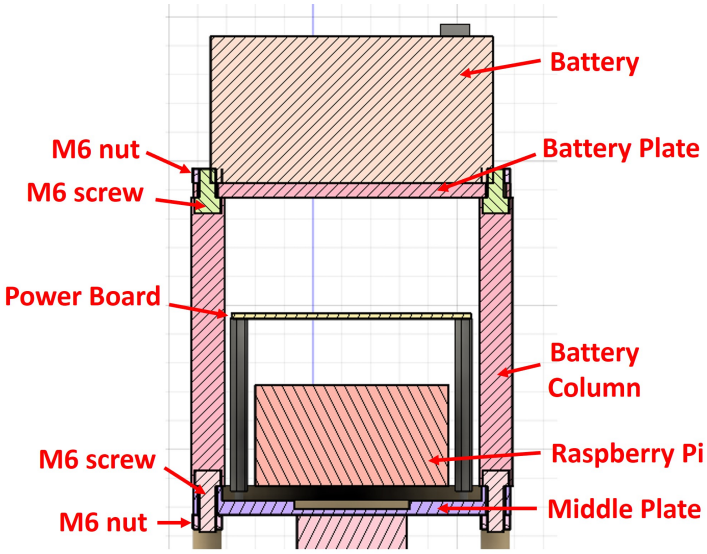

Figure 21: The cross-section of the Middle Plate and the Battery Plate.

2.1 Summary

In summary, we built a low-cost and quick-release device that captures images from the top. To study the angular momentum of rotating/non-rotating plasma disks, top-view cameras play an important role in this study. Figure 22 shows the image captured by the top-view camera. Although we are using aluminum plates to form the Faraday cage to resist electromagnetic pulses, the top view camera is still crashed in experiments. For that, we will solve the top-view camera crash problem and use it to study the angular momentum of the plasma disk.

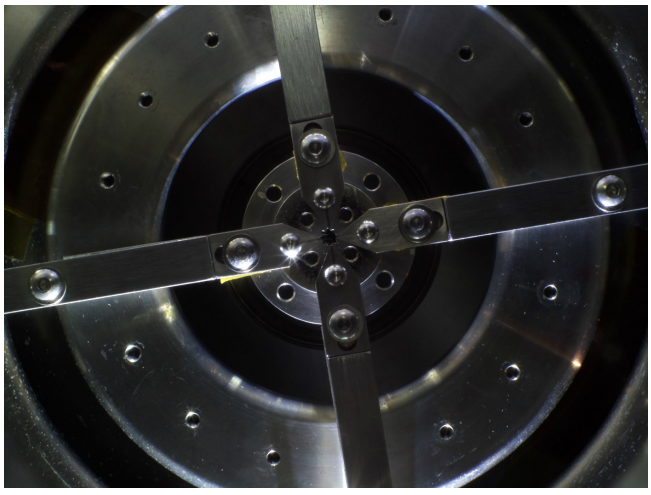

Figure 22: The image captured from the top-view camera.

3 The optical table system

The optical table is mainly used to set up the optical path of the laser. I built two subsystems of the optic table. One is the Fan Filter Unit (FFU). The other is the Light-Emitting Diode (LED) light. The FFU is the air conditioning system, keeping the air circulating and keeping optical elements clean. The optical table FFU will be presented in section 3.1. The optical table lighting system uses a pair of 1-m LED strip lights. The LED strip light is controlled by a switch box, which has two switches and four channels. The LED switch box will be introduced in chapter 3.2.

3.1 The Fan-Filter Unit (FFU)

Our laboratory has two sets of FFU systems, one is the dust-free cabinet[2], and the other one is an air conditioning system for the optical table. All FFU systems use single phase 220-volt power from the same plug. Each FFU system has a set of power switches and pilot lamps. The pilot lamp is used to indicate if the power is on. Figure 23(a) shows the power switch and pilot lamp in the FFU system. The optical-table FFU system has another switch on the control panel as shown in figure 24(a). Figure 23(b) is circuit digram of the FFU systems. The optical-table FFU system is completed and operational.

(a) (b)

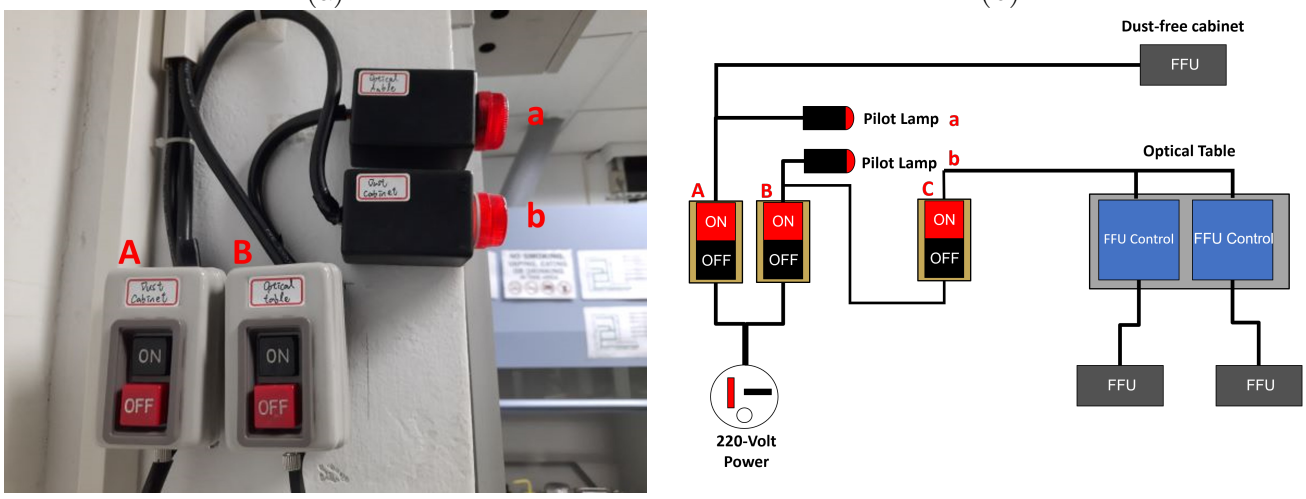

Figure 23: (a) The power switch and pilot lamp (b) The circuit diagram of FFU system

3.2 The Light-Emitting Diode (LED) light strip

The lighting system of the optical table uses LED light strips. The switch box has two switches to control the north and the south LED light strips. The LED light strips are powered by 12-V power supply. Each switch can control one LED light strip. Figure 24(a) is the control panel with the LED switch box and the FFU switch. Figure 24(b) is the optical LED light strip in operation. The circuit diagram is shown in figure 24(c). In conclusion, the air conditioning system and the light system of the optical table have been completed and operational.

(a) (b) (c)

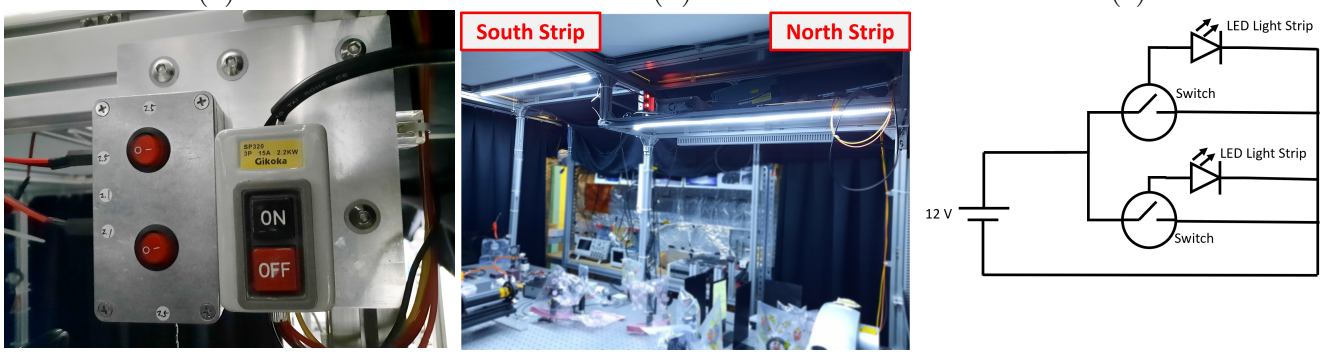

Figure 24: (a) The control panel (b) The LED light strips (c) The circuit diagram of the switch box

4 Future work

We found an asymmetry problem with bi-conical-wire array. Further, we observed that the tungsten wires of the upper conical-wire array was darker than the lower conical-wire array. Figure 25(a)-(b) showns the gray value profile of the tungsten wire of the lower conical-wire array and upper conical-wire array, respectively. For this reason, we assume that the current cannot be efficiently delivered to the upper conical-wire array. Therefore, we replaced the Middle layer of the bi-conical-wire array with an insulating material such as Polylactide. Figure 26 shows the CAD drawing of the bi-conical-wire array with the metal top disk and the insulating middle layer. Table 3 shows the bi-conical-wire array with different components in experiments. Figure 27(a)-(c) show the visible-light images of different experiments. The bi-conical-wire with the metal top disk and the insulating middle layer has a plasma plume at the upper conical-wire array. Therefore, we can study the different versions bi-conical-wire array to solve the asymmetry problem. On the other hand, the top-view camera crashed in the experiment. In the future, we will solve this technical problem and use the top-view camera to study the angular momentum evolution of the plasma disk.

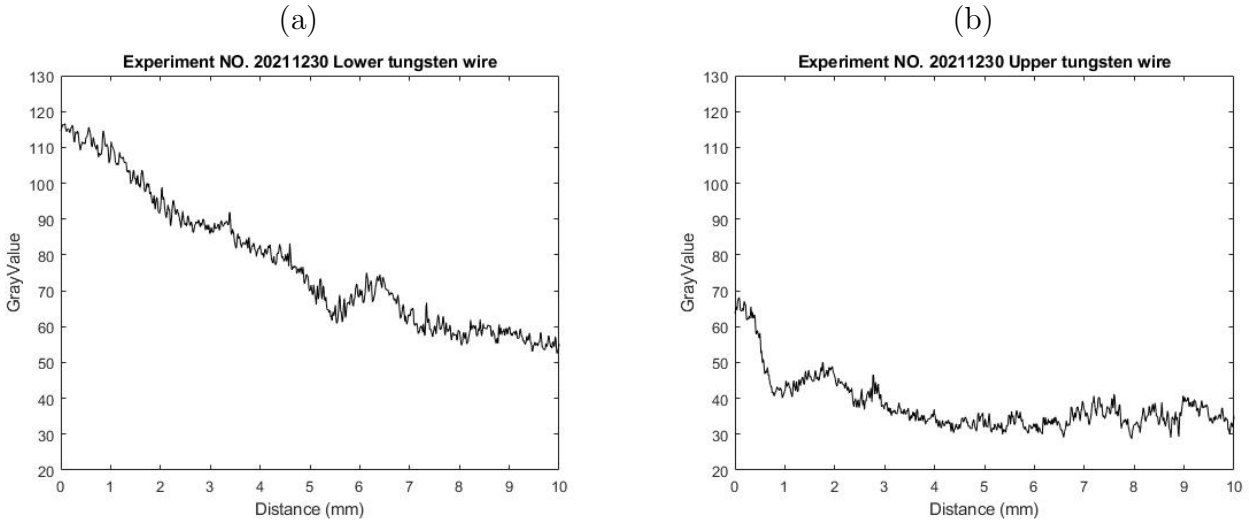

Figure 25: (a) The gray value profile of the lower tungsten wire. (b) The gray value profile of the upper tungsten wire.

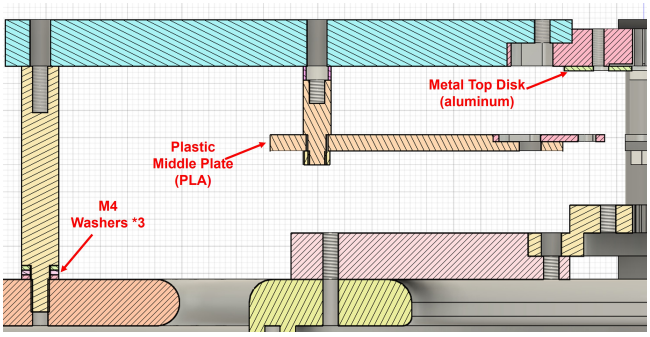

Figure 26: The bi-conical-wire array with insulated middle layer and metal top disk.

Table 3: The different version of bi-conical-wire array.

Experiment NO.	20211230	20220217	20220224
Insulating Middle layer	None	Yes	Yes
Metal Top disk	None	None	Yes

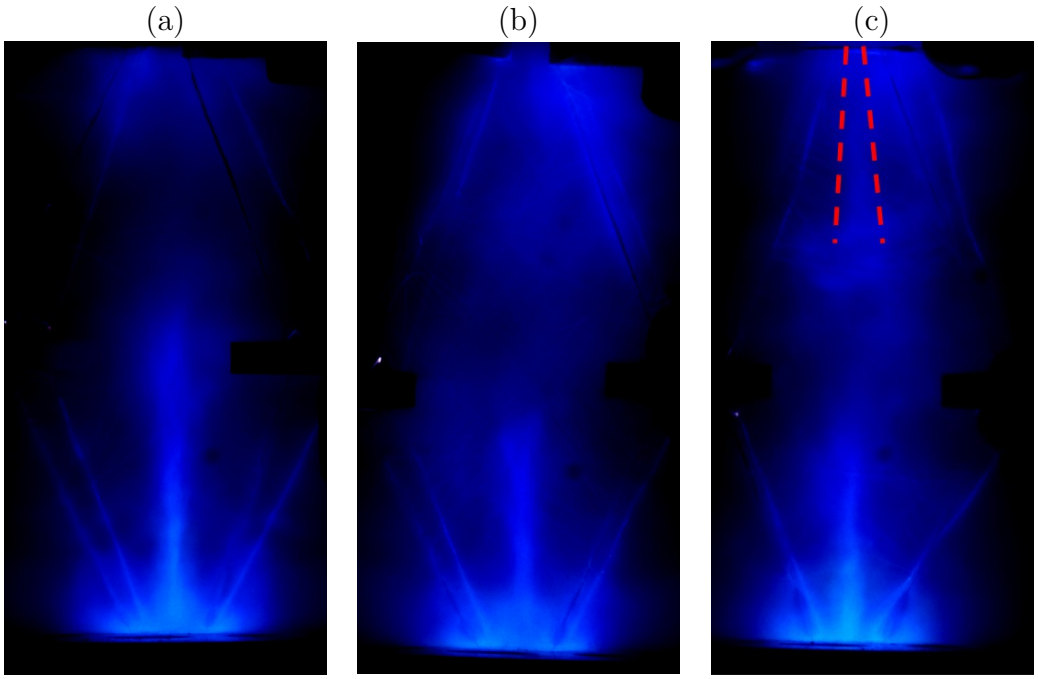

Figure 27: (a) The image of experiment NO. 20211230. (b) The image of experiment NO. 20220217. (c) The image of experiment NO. 20220224.

5 Summary

We built the Jet-velocity measurement system to measure the plasma jet velocity. The measured plasma-jet velocity was ∼90 km/s. Next, we built the bi-conical-wire array to study the two counter-propagate plasma jets colliding with each other. Further, I built the top-view to the visible-light camera system. The visible light time-integrated image from the top plays an important role in the study of the plasma disk. For the laser camera system, the optical table system is completed and operational. In the future, we will study the rotating/non-rotating plasma disk and use the interferometer to measure the density of the plasma.

References

[1] Po-Yu Chang etc. One-kilojoule Pulsed-power Generator for Laboratory Space Sciences. *Rev. Sci. Instrum.*, 93, April 2022.

[2] Yen-Cheng Lin. Studies of rotating plasma jets produced by twisted-conical-wire arrays. Master's thesis, National Cheng Kung University Institute of Space and Plasma Science, 2021.

[3] https://www.thorlabs.com/thorproduct.cfm?partnumber=fp400urt.

[4] https://www.thorlabs.com/thorproduct.cfm?partnumber=ft030.

[5] https://www.thorlabs.com/thorproduct.cfm?partnumber=det10a2.

[6] A. Ciardi S. C. Bott G. N. Hall N. Naz C. A. Jennings M. Sheriock J. P. Chittenden J. B. A. Palmer A. Frank D. J. Ampleford, S. V. Lebedev and E. Blackman. Supersonic Radiatively Cooled Rotating Flows and Jets in the Laboratory. *Phys Rev Lett*, 100:3–25, January 2008.

[7] https://twcn.rsonline.com/web/p/raspberry-pi/1822098/.

[8] https://twcn.rsonline.com/web/p/raspberry-pi-cameras/2012852.

A Appendix

A.1 The CAD drawing of the LensHolder

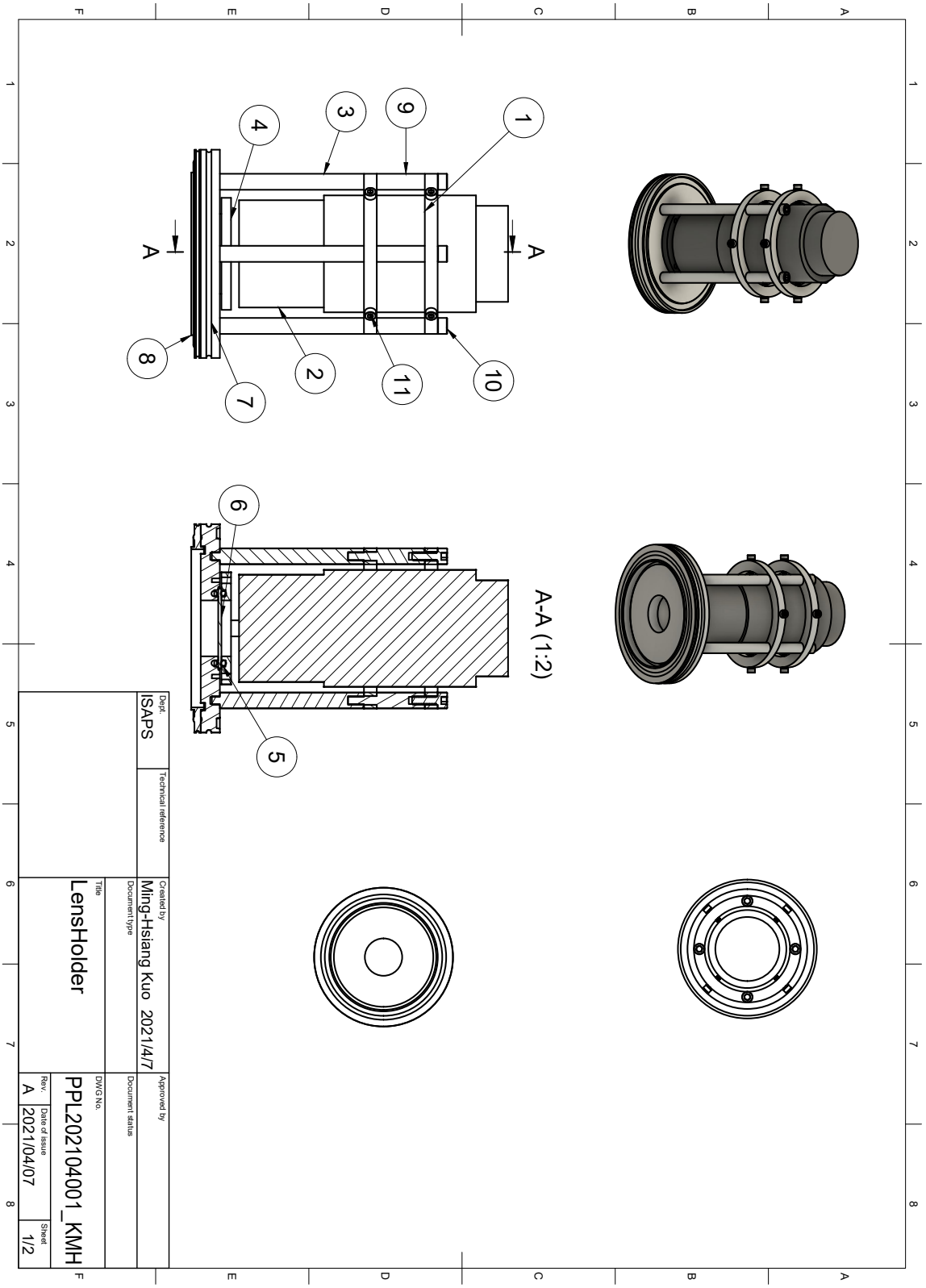

Parts List				
Item	Qty	Part Number	Description	Material
1	2	PPL202104002_KMH	RingHolder	Stainless Steel
2	1	Nikon AF NIKKOR 70-300mm	Lens	Stainless Steel
3	4	PPL202104003_KMH	Foot_Flange_Lens	Stainless Steel
4	1	PGS202011004_CPU	TopPlate	Stainless Steel
5	2	Oring_P40		Rubber
6	1	PGS201908038_CPU	Window	Glass
7	1	PGS202011003_CPU	ISO100_CameraHolder	Stainless Steel
8	1	ISO100CenterRing		Stainless Steel
9	4	PPL202104004_KMH	Foot_LensHolder	Stainless Steel
10	4	M6 16mm		Stainless Steel
11	8	M4 14mm		Stainless Steel

Dept.	Technical reference	Created by	Approved by
ISAPS		Ming-Hsiang Kuo 2021/4/7	
		Document type	Document status
		Title: LensHolder	DWG No.: PPL202104001_KMH
		Rev.: A	Date of issue: 2021/04/07 — Sheet: 2/2

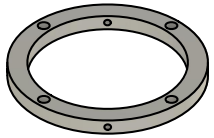

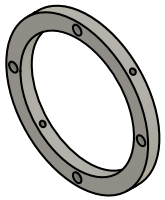

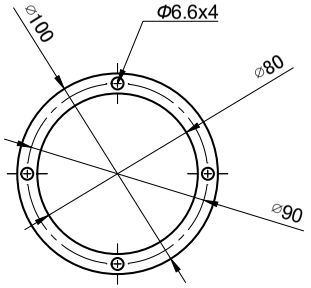

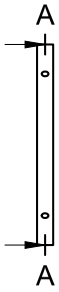

A-A (1:2)

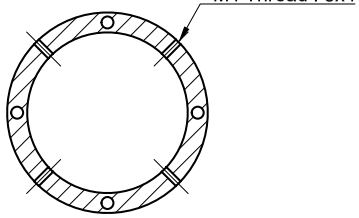

Unit: mm

Note:
Unless otherwise specified
- Tolerance: 2PL±0.005
- Edge: 0.4 x 45°
- Inside cor rad: 0.4

Dept.	Technical reference	Created by	Approved by
ISAPS		Ming-Hsiang Kuo 2021/4/8	
		Document type	Document status
		Title: LensHolder RingHolder	DWG No.: PPL202104002_KMH
			Rev.: A / Date of issue: 2021/04/08 / Sheet: 1/1

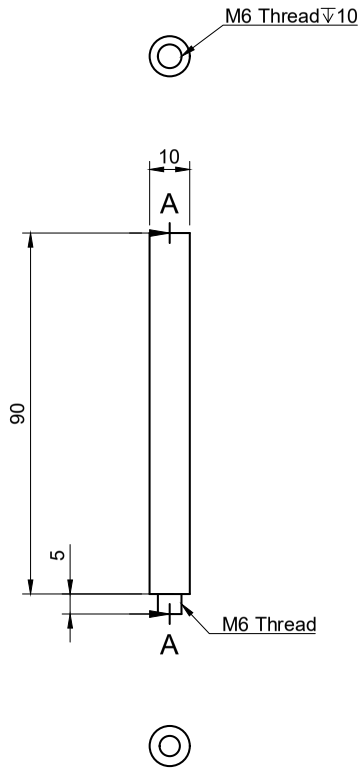

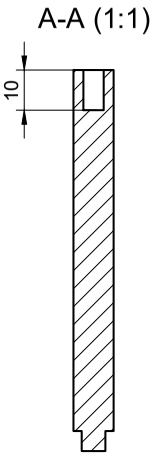

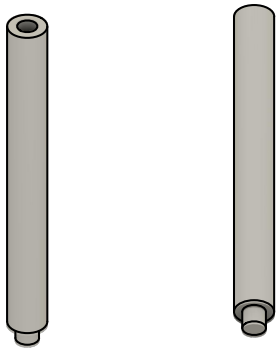

Unit: mm

Note:
Unless otherwise specified
- Tolerance: 2PL±0.005
- Edge: 0.4 x 45°
- Inside cor rad: 0.4

Dept.	Technical reference	Created by	Approved by
ISAPS		Ming-Hsiang Kuo 2021/4/7	
		Document type	Document status
		Title: LensHolder Foot_Flange_Lens	DWG No.: PPL202104003_KMH
			Rev.: A / Date of issue: 2021/04/07 / Sheet: 1/1

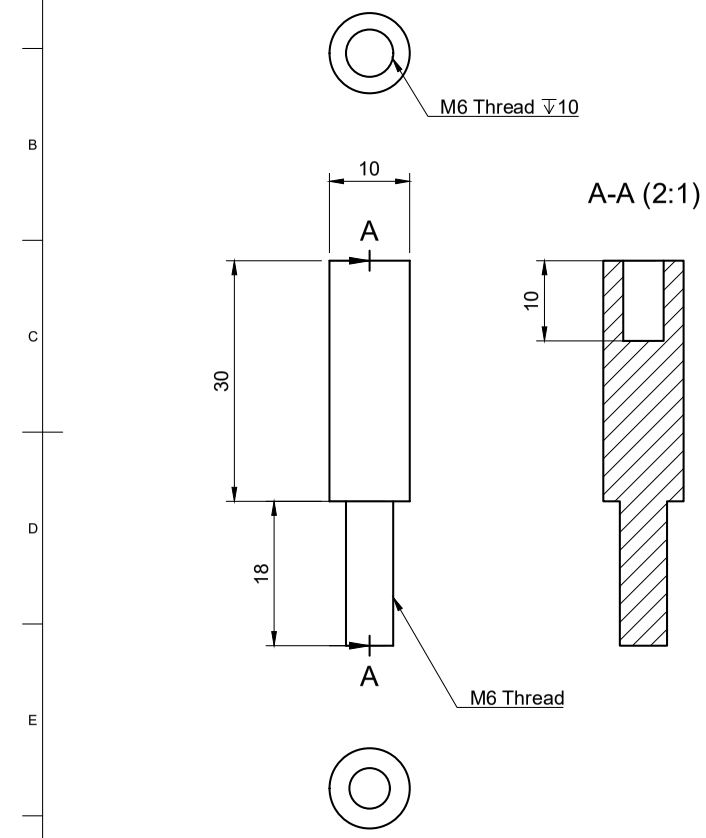

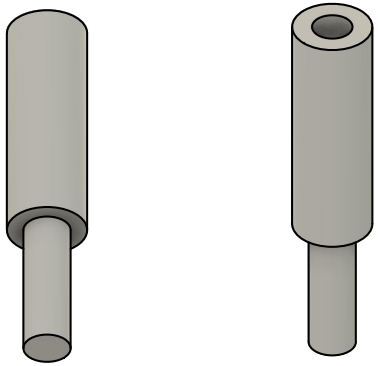

Unit: mm

Note:
Unless otherwise specified
- Tolerance: 2PL±0.005
- Edge: 0.4 x 45°
- Inside cor rad: 0.4

Dept.	Technical reference	Created by	Approved by
ISAPS		Ming-Hsiang Kuo 2021/4/7	
		Document type	Document status
		Title: LensHolder Foot_LensHolder	DWG No.: PPL202104004_KMH
			Rev.: A / Date of issue: 2021/4/7 / Sheet: 1/1

A.2 The CAD drawing of the HolderSupport

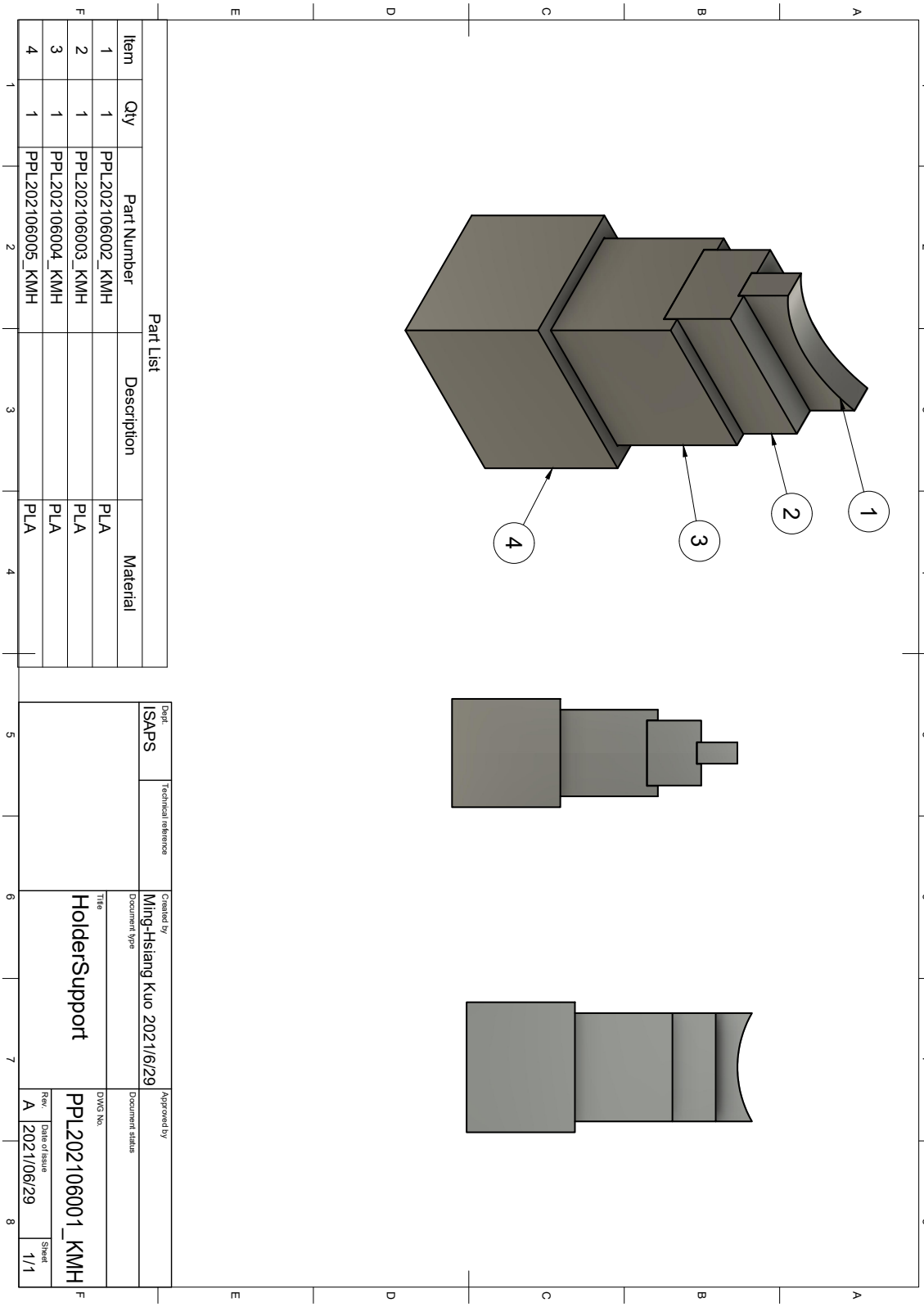

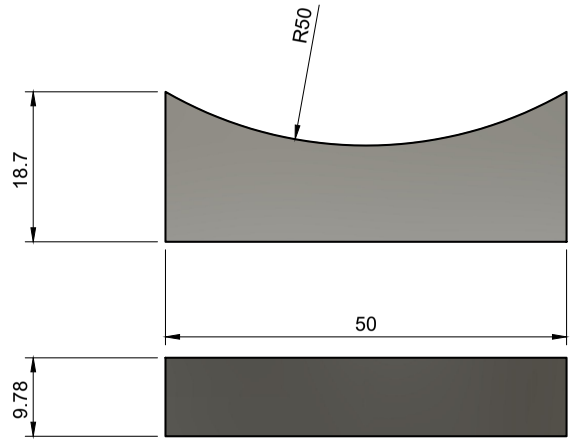

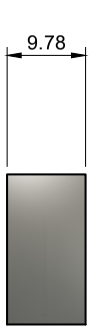

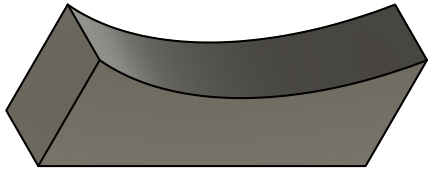

Unit: mm

Note:

- **3D Printer Manufacture**
- **PLA Material**

Dept.	Technical reference	Created by	Approved by
ISAPS		Ming-Hsiang Kuo 2021/4/27	
		Document type	Document status
		Title: TopHolder	DWG No.: PPL202106002_KMH
			Rev.: A / Date of issue: 2021/06/29 / Sheet: 1/1

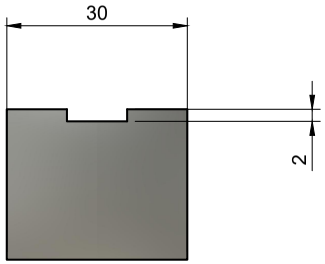

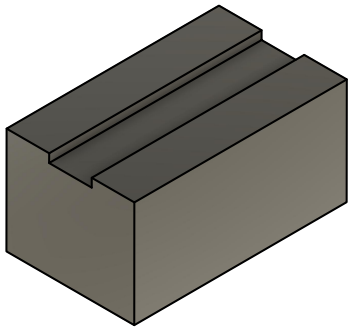

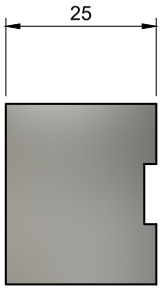

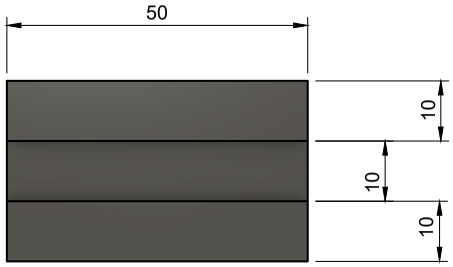

Unit: mm

Note:

- **3D Printer Manufacture**
- **PLA Material**
- **3D Printer Hollow Shrink: -0.3**

E.g
Disgn:Ø10,Actual:Ø9.7

Dept.	Technical reference	Created by	Approved by
ISAPS		Ming-Hsiang Kuo 2021/6/29	
		Document type	Document status
		Title: MiddleHolder	DWG No.: PPL202106003_KMH
			Rev.: A / Date of issue: 2021/06/29 / Sheet: 1/1

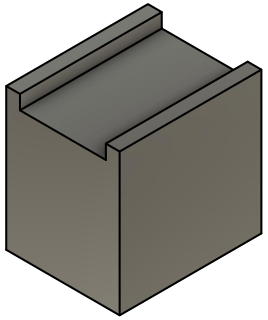

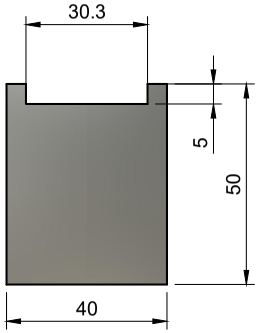

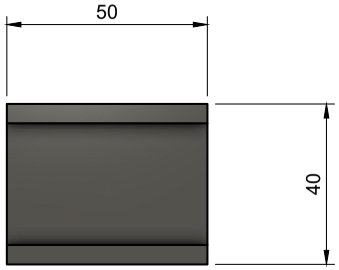

Unit: mm

Note:

- **3D Printer Manufacture**
- **PLA Material**
- **3D Printer Hollow Shrink: -0.3**

E.g
Disgn:30.3,Actual:30

Dept.	Technical reference	Created by	Approved by
ISAPS		Ming-Hsiang Kuo 2021/6/29	
		Document type	Document status
		Title: ButtomHolder	DWG No.: PPL202106004_KMH
			Rev.: A / Date of issue: 2021/06/29 / Sheet: 1/1

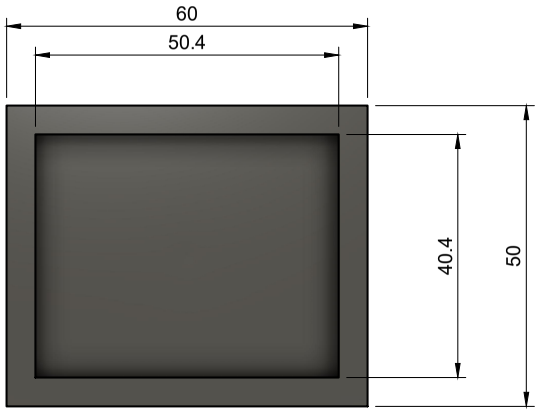

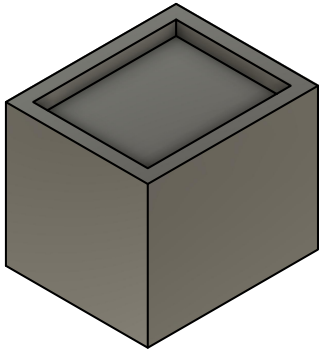

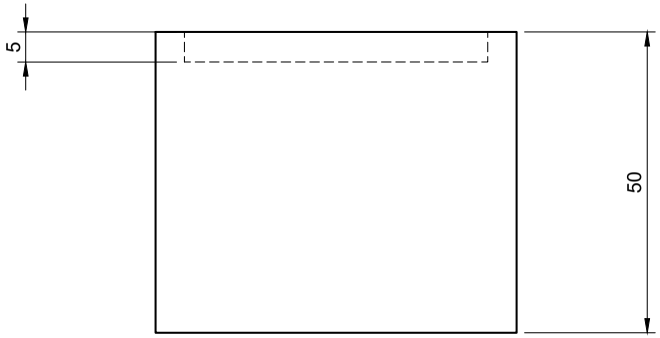

Unit: mm

Note:

- **3D Printer Manufacture**
- **PLA Material**
- **3D Printer Notch Shrink: -0.4**

E.g
Disgn:40.4,Actual:40

Dept.	Technical reference	Created by	Approved by
ISAPS		Ming-Hsiang Kuo 2021/6/29	
		Document type	Document status
		Title: BaseSupport	DWG No.: PPL202106005_KMH
			Rev.: A / Date of issue: 2021/06/29 / Sheet: 1/1

A.3 The CAD drawing of the FiberHolder

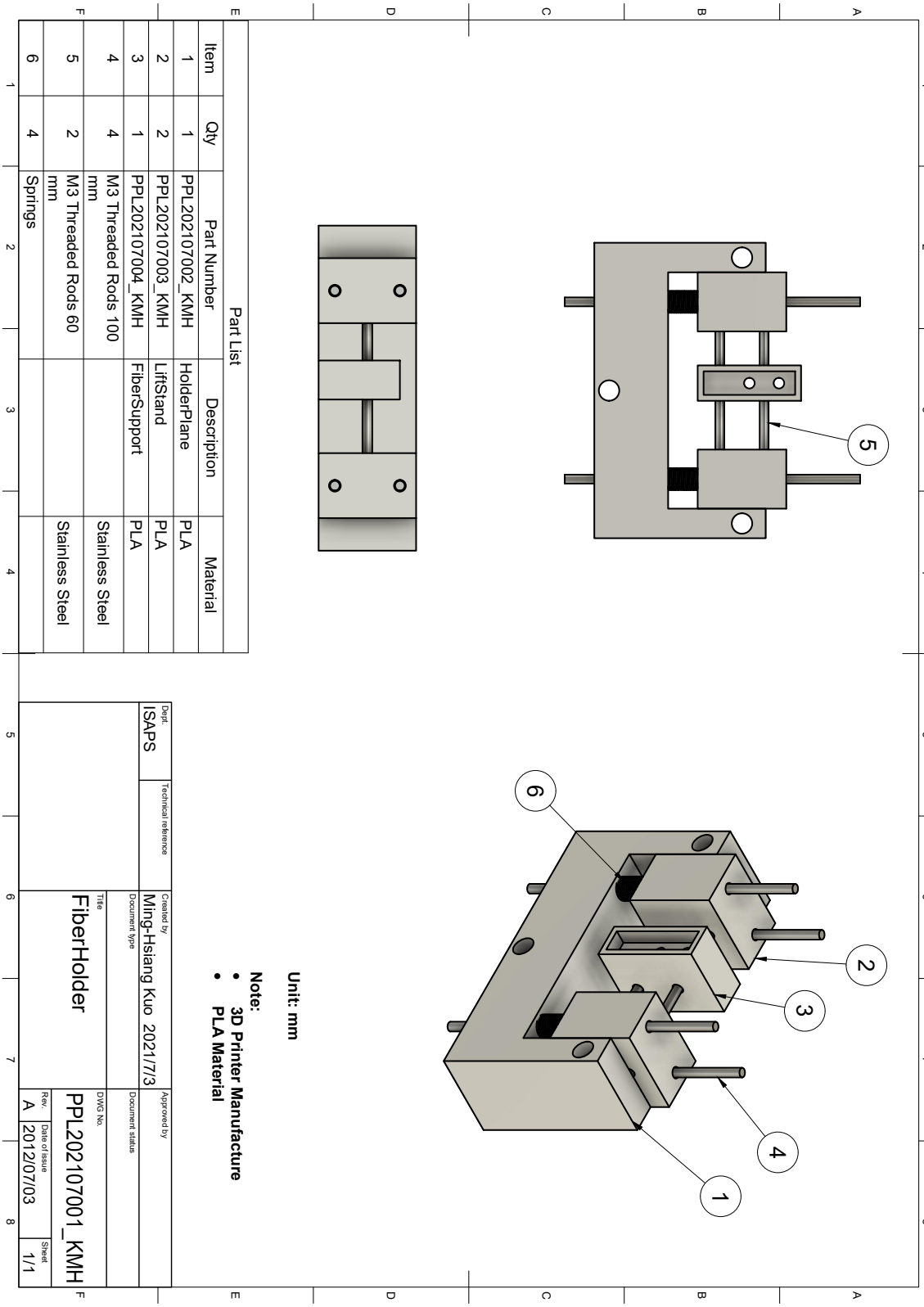

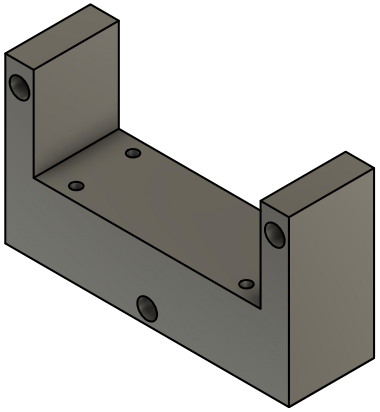

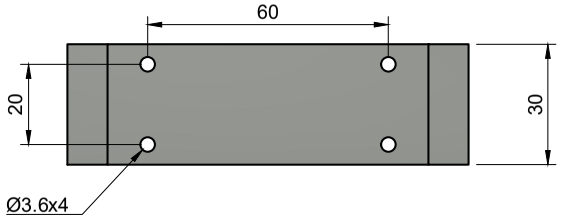

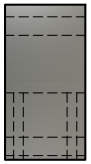

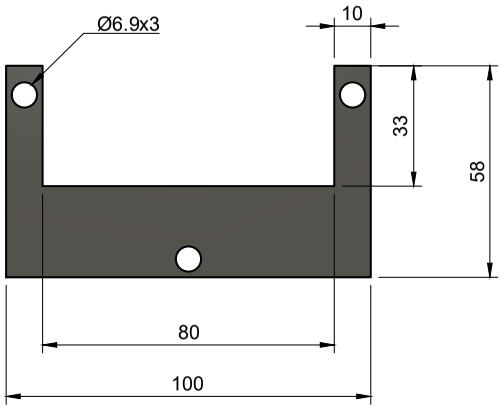

Unit: mm

Note:

- **3D Printer Manufacture**
- **PLA Material**
- **3D Printer Hole Shrink: -0.3**

E.g
Disgn:Ø3.6,Actual:Ø3.3

Dept.	Technical reference	Created by	Approved by
ISAPS		Ming-Hsiang Kuo 2021/7/03	
		Document type	Document status
		Title: HolderPlane	DWG No.: PPL202107002_KMH
		Rev.: A	Date of issue: 2021/07/03 — Sheet: 1/1

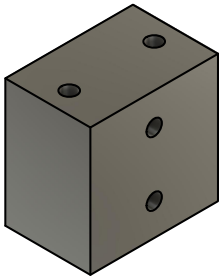

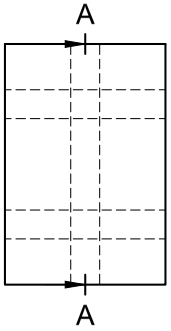

A-A (2:1)

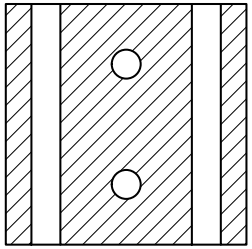

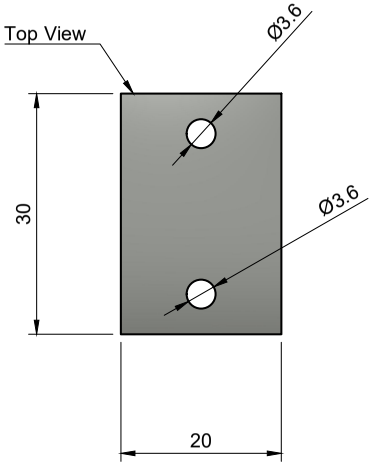

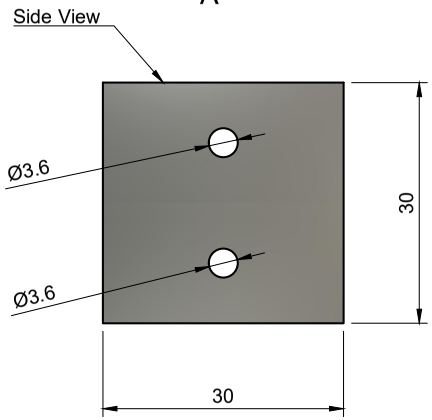

Unit: mm

Note:

- **3D Printer Manufacture**
- **PLA Material**
- **3D Printer Hole Shrink: -0.3**

E.g
Disgn:Ø3.6,Actual:Ø3.3

Dept.	Technical reference	Created by	Approved by
ISAPS		Ming-Hsiang Kuo 2021/7/03	
		Document type	Document status
		Title: LiftStand	DWG No.: PPL202107003_KMH
		Rev.: A	Date of issue: 2021/07/03 — Sheet: 1/1

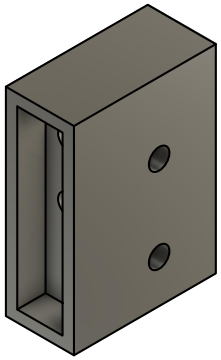

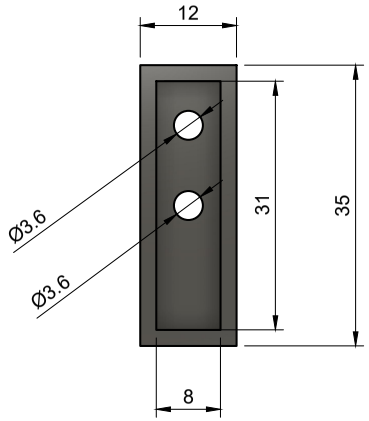

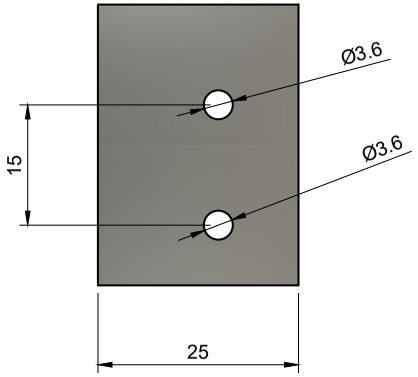

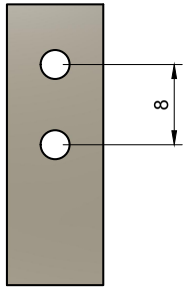

A-A (2:1)

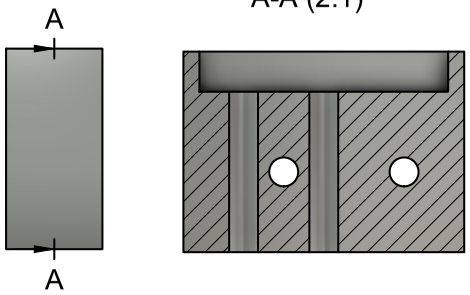

Unit: mm

Note:

- **3D Printer Manufacture**
- **PLA Material**
- **3D Printer Hole Shrink: -0.3**

E.g
Disgn:Ø3.6,Actual:Ø3.3

Dept.	Technical reference	Created by	Approved by
ISAPS		Ming-Hsiang Kuo 2021/7/03	
		Document type	Document status
		Title: FiberSupport	DWG No.: PPL202107004_KMH
			Rev.: A / Date of issue: 2021/07/03 / Sheet: 1/1

A.4 The CAD drawing of the AlignmentStand

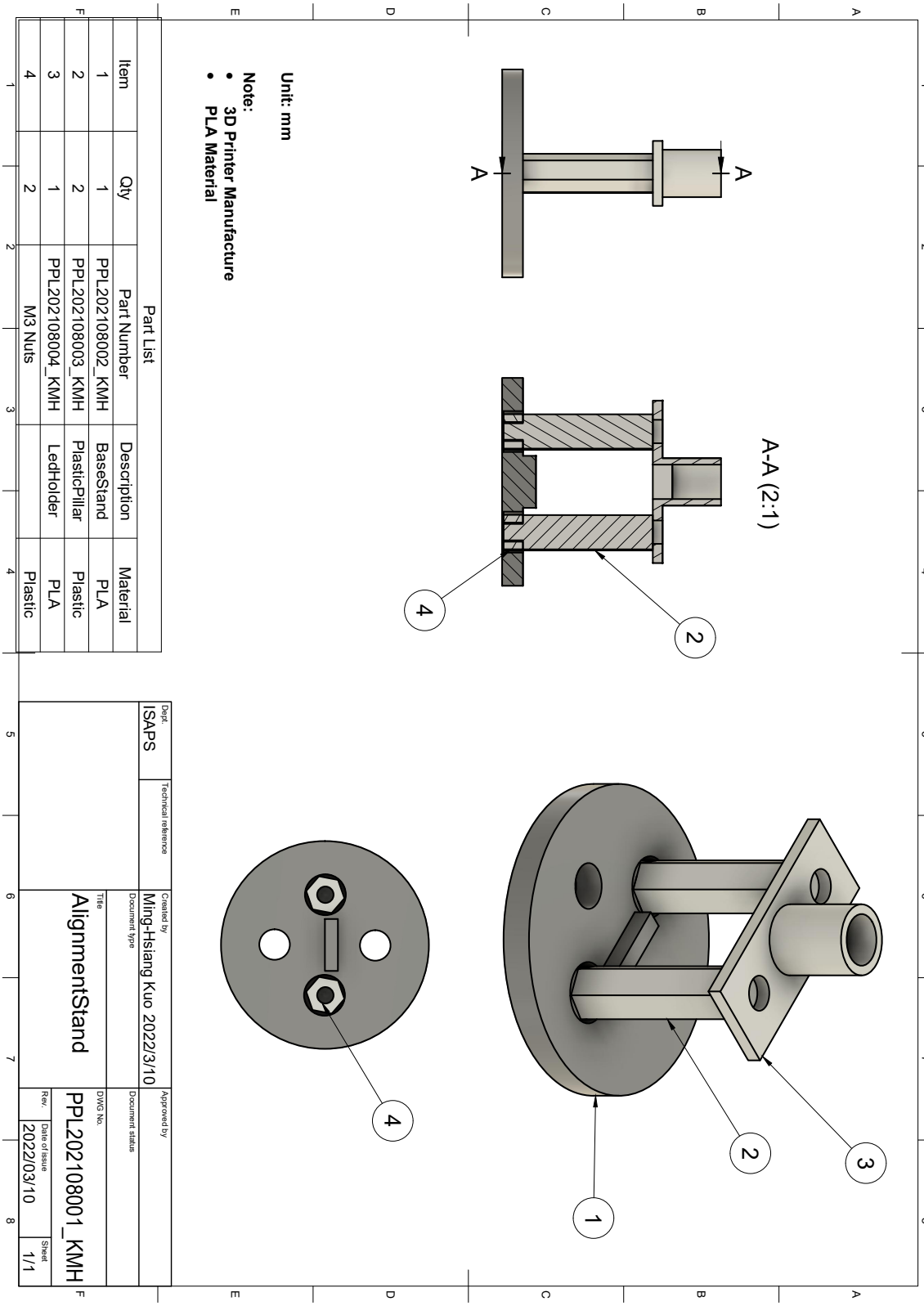

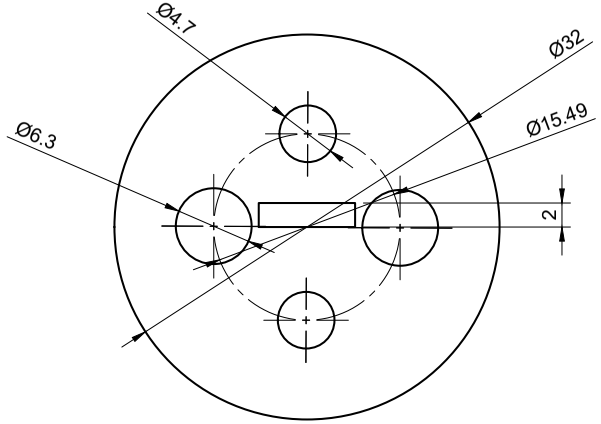

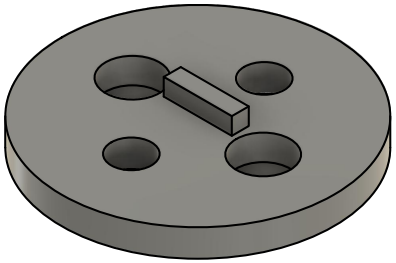

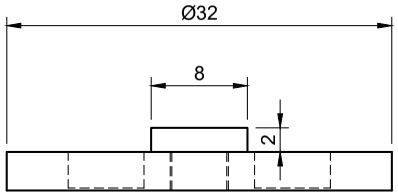

Unit: mm

Note:

- **3D Printer Manufacture**
- **PLA Material**
- **3D Printer Hole Shrink: -0.3**

E.g
Disgn:Ø6.3,Actual:Ø6.0

Dept.	Technical reference	Created by	Approved by
ISAPS		Ming-Hsiang Kuo 2022/3/10	
		Document type	Document status
		Title: BaseStand	DWG No.: PPL202108002_KMH
		Rev.	Date of issue: 2022/03/11 — Sheet: 1/1

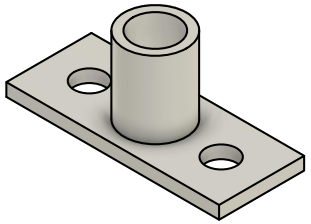

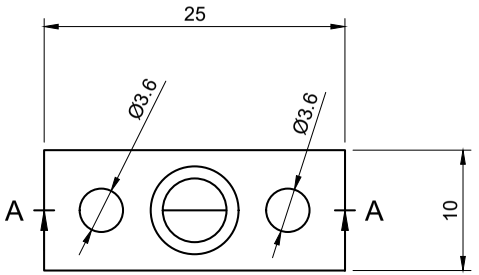

A-A (3:1)

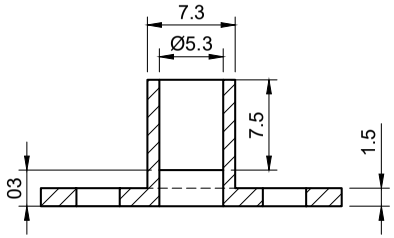

Unit: mm

Note:

- **3D Printer Manufacture**
- **PLA Material**
- **3D Printer Hole Shrink: -0.3**

E.g
Disgn:Ø5.3,Actual:Ø5

Dept.	Technical reference	Created by	Approved by
ISAPS		Ming-Hsiang Kuo 2021/7/20	
		Document type	Document status
		Title: LedHolder	DWG No.: PPL202108003_KMH
		Rev.	Date of issue: 2022/03/11 — Sheet: 1/1

A.5 The PowerBoard Layout for the AlignmentStand

A.6 The CAD drawing of the bi-conical-wire array

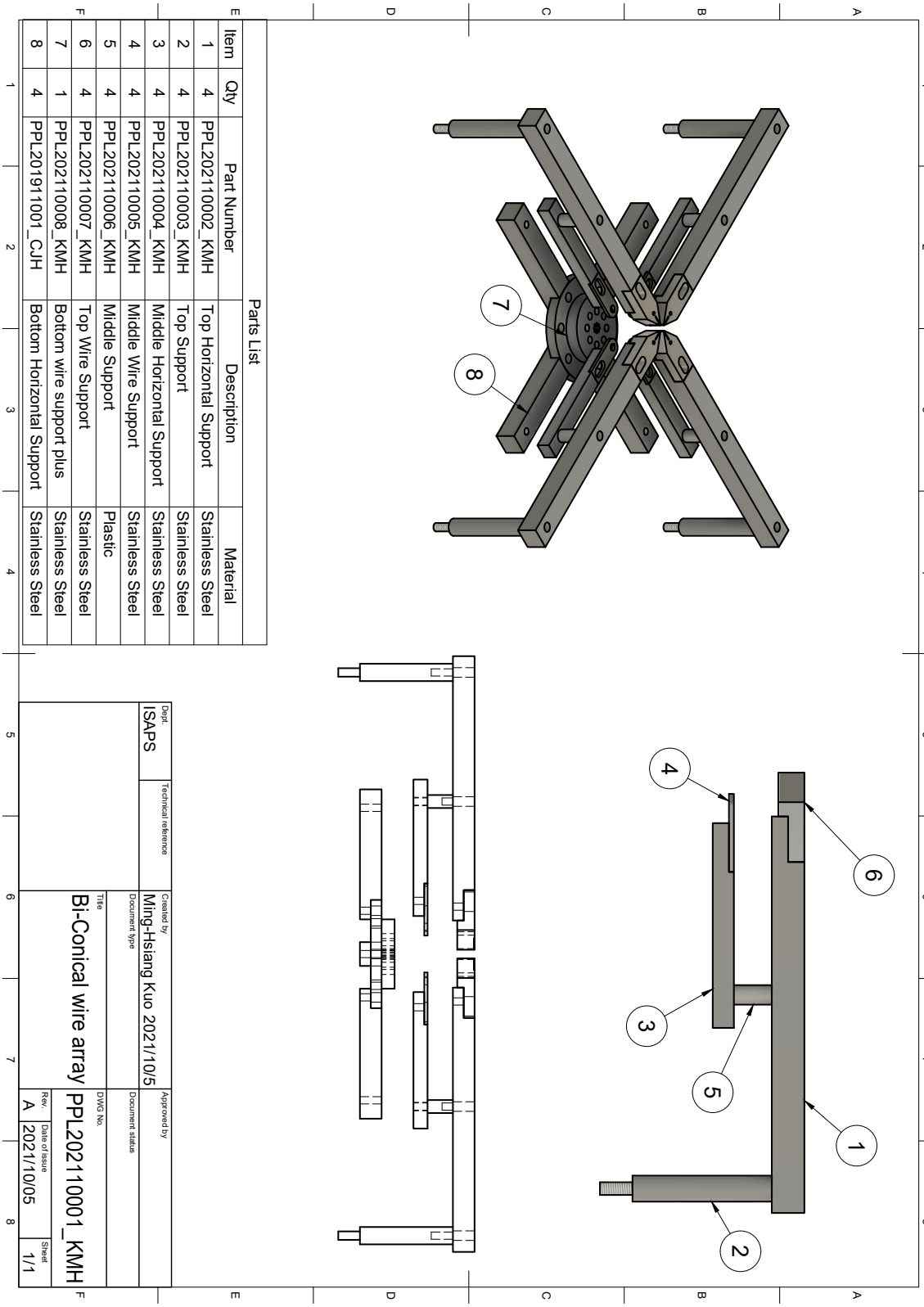

Parts List

Item	Qty	Part Number	Description	Material
1	4	PPL202110002_KMH	Top Horizontal Support	Stainless Steel
2	4	PPL202110003_KMH	Top Support	Stainless Steel
3	4	PPL202110004_KMH	Middle Horizontal Support	Stainless Steel
4	4	PPL202110005_KMH	Middle Wire Support	Stainless Steel
5	4	PPL202110006_KMH	Middle Support	Plastic
6	4	PPL202110007_KMH	Top Wire Support	Stainless Steel
7	1	PPL202110008_KMH	Bottom wire support plus	Stainless Steel
8	4	PPL201911001_CJH	Bottom Horizontal Support	Stainless Steel

Dept. ISAPS | Technical reference | Created by Ming-Hsiang Kuo 2021/10/5 | Approved by

Document type | Document status

Title: Bi-Conical wire array | DWG No. PPL202110001_KMH

Rev. A | Date of issue 2021/10/05 | Sheet 1/1

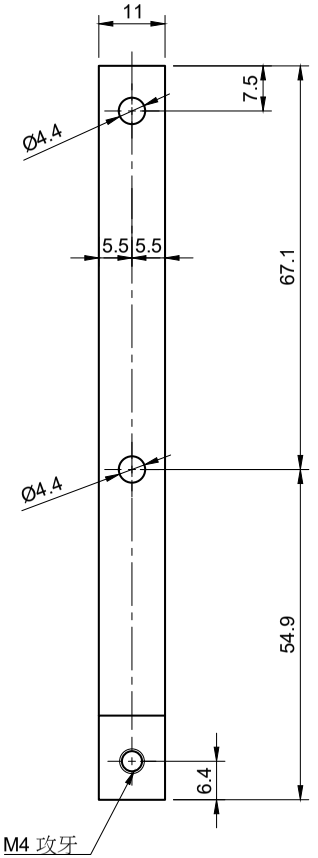

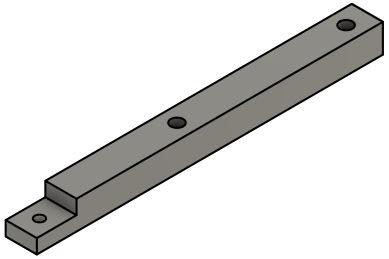

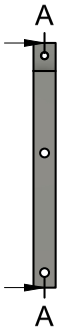

A-A (1:2)

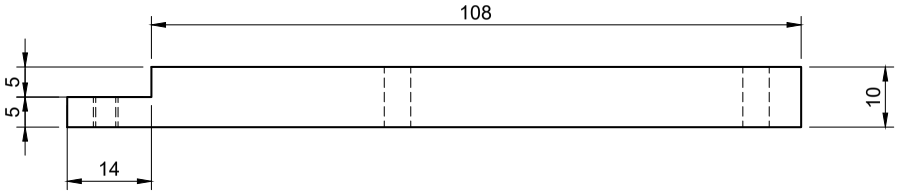

Unit: mm

Note:
Unless otherwise specified
- Tolerance: 2PL±0.005
- Edge: 0.4 x 45°

Dept. ISAPS	Technical reference	Created by Ming-Hsiang Kuo 2021/10/5	Approved by
		Document type	Document status
		Title: Top Horizontal Support	DWG No.: PPL202110002_KMH
		Rev. A	Date of issue 2021/10/05 / Sheet 1/1

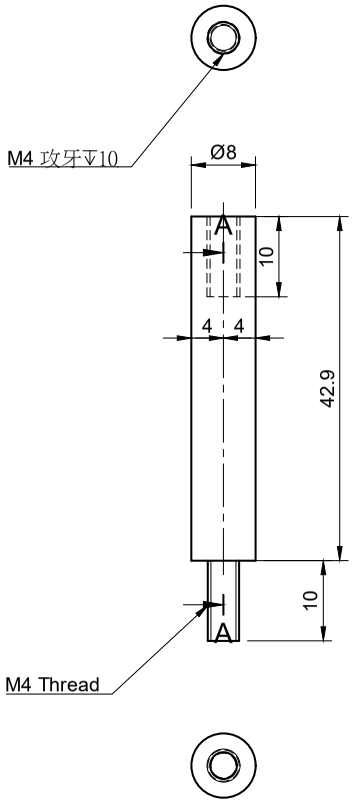

A-A (2:1)

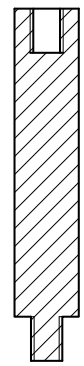

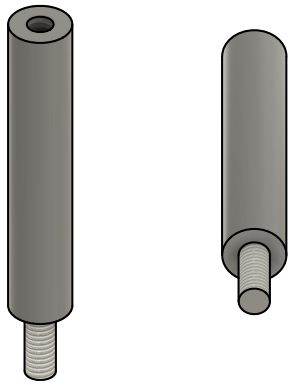

Unit: mm

Note:
Unless otherwise specified
- Tolerance: 2PL±0.005
- Edge: 0.4 x 45°

Dept.	Technical reference	Created by	Approved by
ISAPS		Ming-Hsiang Kuo 2021/10/5	
		Document type	Document status
		Title: Top Support	DWG No.: PPL202110003_KMH
			Rev.: A / Date of issue: 2021/10/05 / Sheet: 1/1

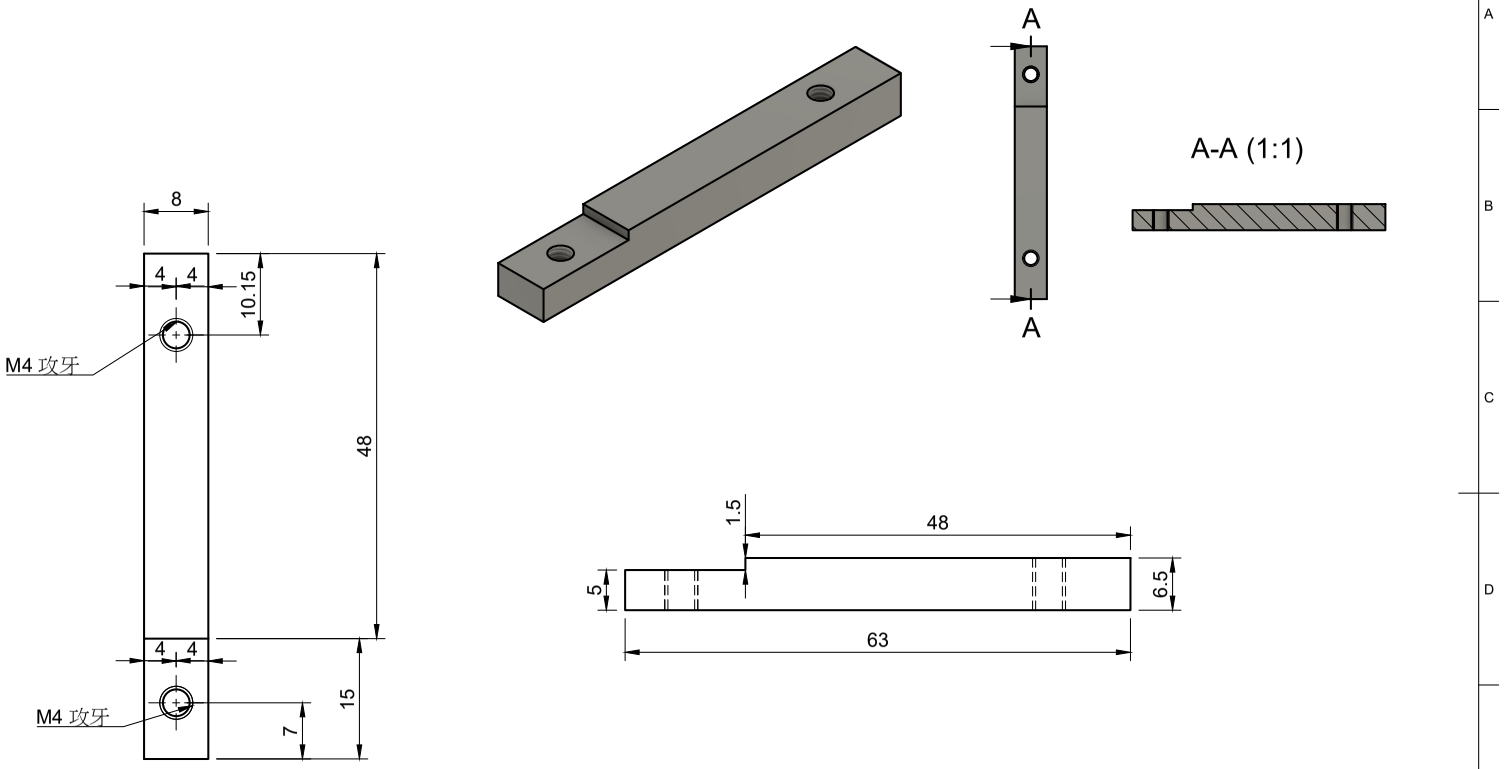

Unit: mm

Note:
Unless otherwise specified
- Tolerance: 2PL±0.005
- Edge: 0.4 x 45°

Dept.	Technical reference	Created by	Approved by
ISAPS		Ming-Hsiang Kuo 2021/10/5	
		Document type	Document status
		Title: Middle Horizontal Support	DWG No.: PPL20211004_KMH
		Rev.: A	Date of issue: 2021/10/05 — Sheet: 1/1

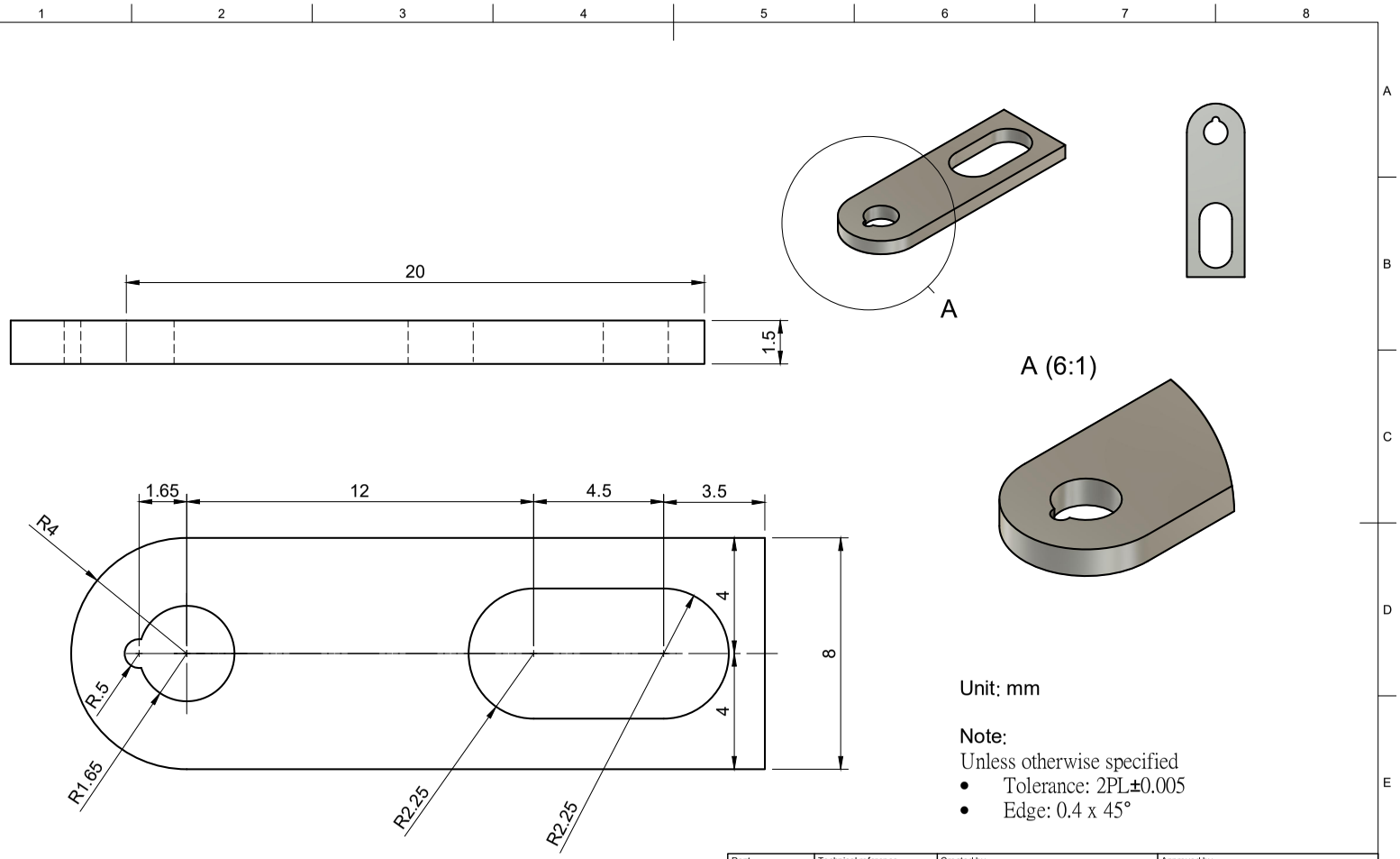

Unit: mm

Note:
Unless otherwise specified
- Tolerance: 2PL±0.005
- Edge: 0.4 x 45°

Dept.	Technical reference	Created by	Approved by
ISAPS		Ming-Hsiang Kuo 2021/10/5	
		Document type	Document status
		Title: Middle Wire Support	DWG No.: PPL202110005_KMH
		Rev.: A	Date of issue: 2021/10/05 — Sheet: 1/1

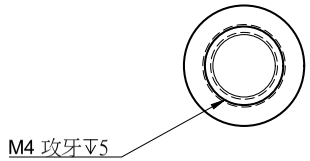

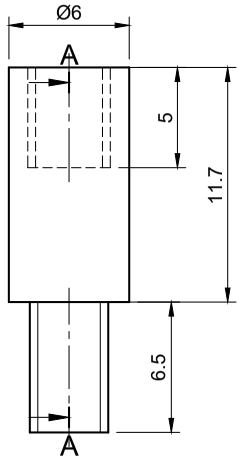

A-A (5:1)

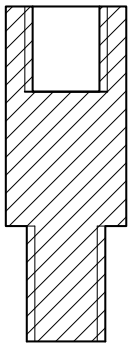

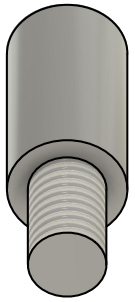

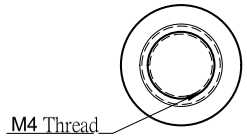

Unit: mm

Note:
Unless otherwise specified

- Tolerance: 2PL±0.005
- Edge: 0.4 x 45°
- Plastic Steel

Dept.	Technical reference	Created by	Approved by	
ISAPS		Ming-Hsiang Kuo 2021/10/5		
		Document type	Document status	
		Title: Middle Support	DWG No.: PPL202110006_KMH	
			Rev.: A / Date of issue: 2021/10/05	Sheet: 1/1

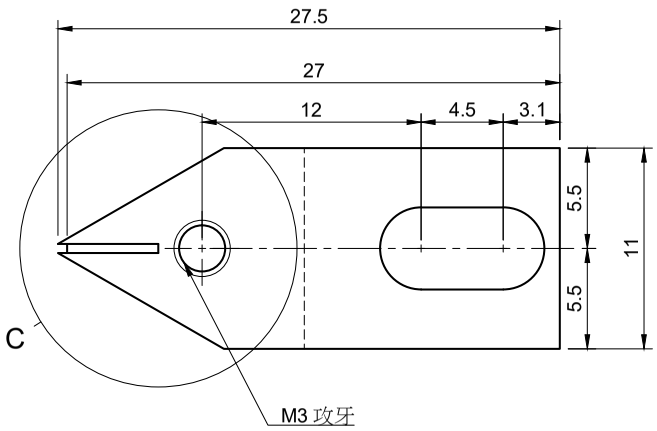

A (5:1)

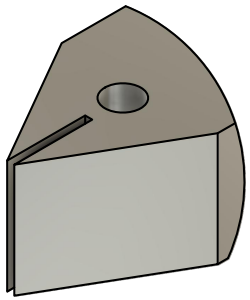

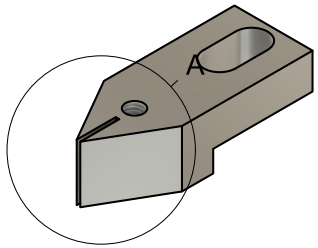

C (5:1)

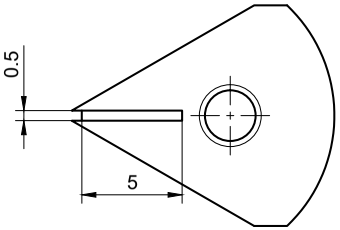

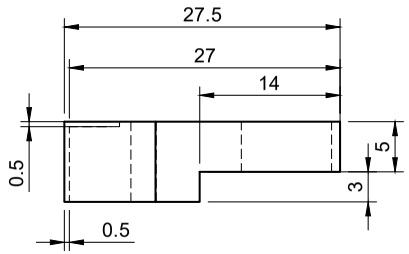

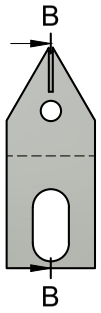

B-B (2:1)

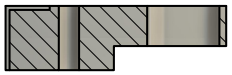

Unit: mm

Note:
Unless otherwise specified
- Tolerance: 2PL±0.005
- Edge: 0.4 x 45°

Dept.	Technical reference	Created by	Approved by
ISAPS		Ming-Hsiang Kuo 2021/10/8	
		Document type	Document status
		Title: Top Wire Support	DWG No.: PPL202110007_KMH
		Rev.: A	Date of issue: 2021/10/08 — Sheet: 1/1

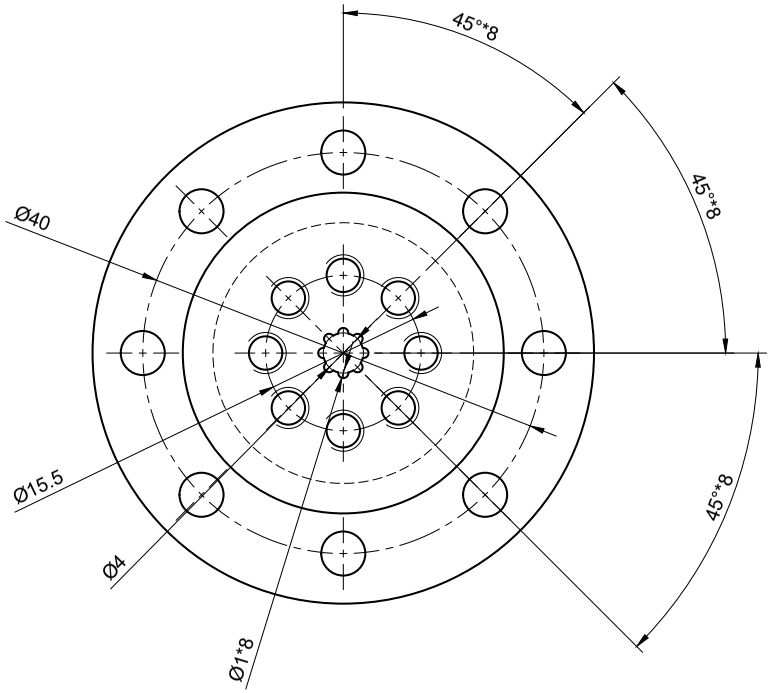

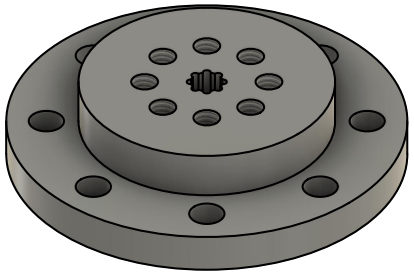

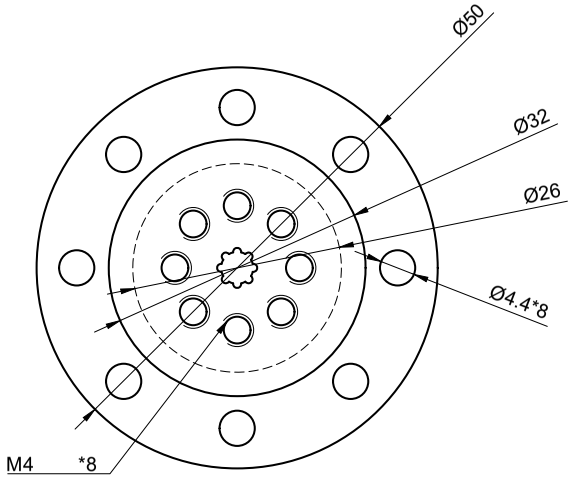

Unit: mm

Note:
Unless otherwise specified
- Tolerance: 2PL±0.005
- Edge: 0.4 x 45°

Dept.	Technical reference	Created by	Approved by
ISAPA		Ming-Hsiang Kuo 2021/10/12	
		Document type	Document status
		Title: Bottom wire support plus	DWG No.: PPL202110008_KMH
		Rev.: A	Date of issue: 2021/10/12
			Sheet: 1/2

A.7 The CAD drawing of the Top-view camera cage

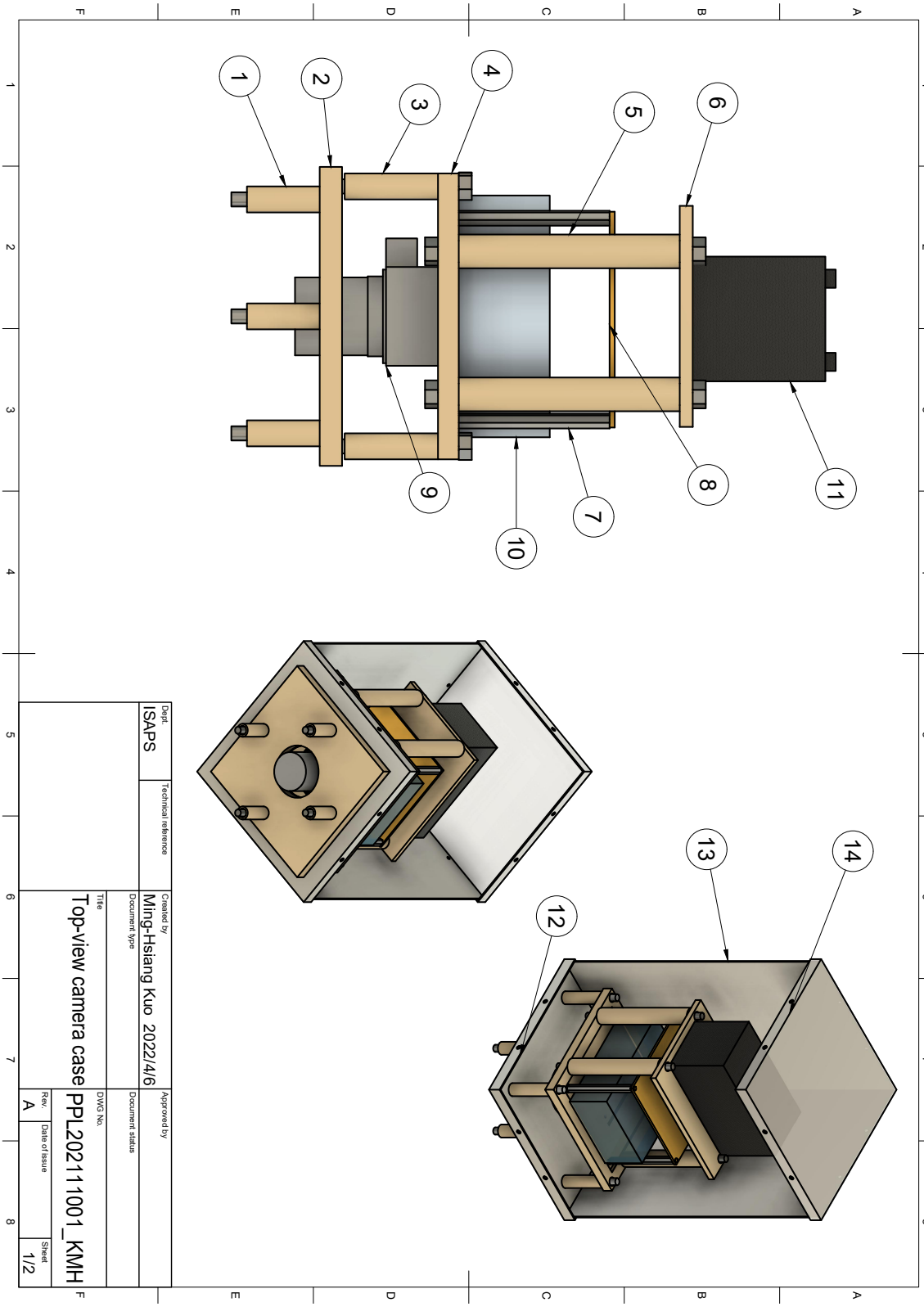

Part List				
Item	Qty	Part Number	Description	Material
1	4	PPL202111002_KMH	Base support 28mm	PLA
2	1	PPL202111003_KMH	Base Plate	PLA
3	4	PPL202111004_KMH	Middle Column 35.9mm	PLA
4	1	PPL202111005_KMH	Middle Plate	PLA
5	4	PPL202111006_KMH	Battery Column 85mm	PLA
6	1	PPL202111007_KMH	Battery Plate	PLA
7	4	Board Screw	Board Screw	
8	1	Power Board	Power Board	
9	1	Camera Module	HQ Camera Module	
10	1	Raspberry Pi	Raspberry Pi 4 B 8G	
11	1	Battery	12V Lead–acid Battery	
12	1	PPL202111008_KMH	Al Bottom	Aluminum
13	4	PPL202111009_KMH	Al Side	Aluminum
14	1	PPL202111010_KMH	Al Top	Aluminum

Dept.	Technical reference	Created by	Approved by
		Ming-Hsiang Kuo 2022/4/6	
		Document type	Document status
		Title: Top view camera case	DWG No.
			Rev. / Date of issue / Sheet: 2/2

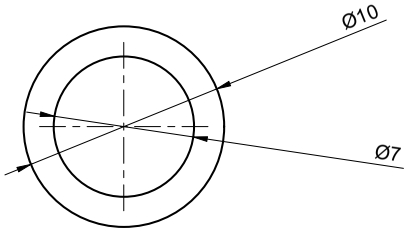

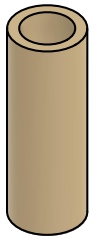

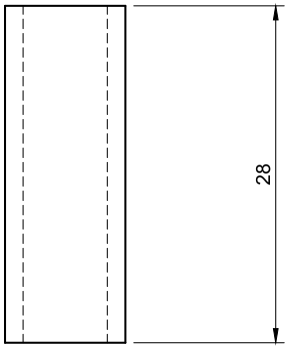

Unit: mm

Note:

- **3D Printer Manufacture**
- **PLA Material**
- **3D Printer Hole Shrink: -0.3**

E.g
Disgn:Ø7.0, Actual:Ø6.7

Dept.	Technical reference	Created by	Approved by
ISAPS		Ming-Hsiang Kuo 2022/4/12	
		Document type	Document status
		Title: Base Support	DWG No.: PPL202111002_KMH
			Rev.: A / Date of issue / Sheet: 1/1

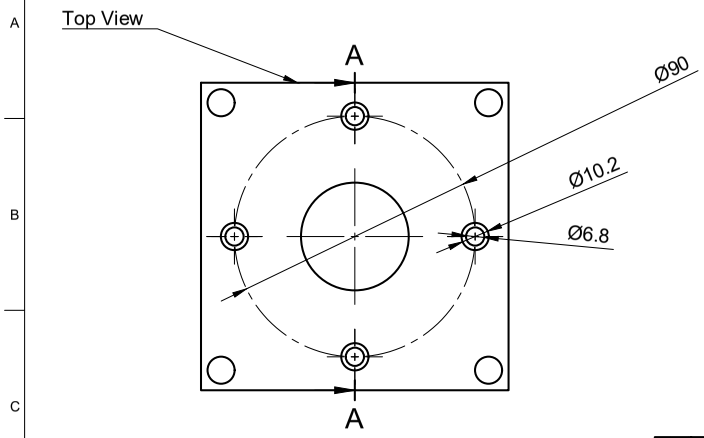

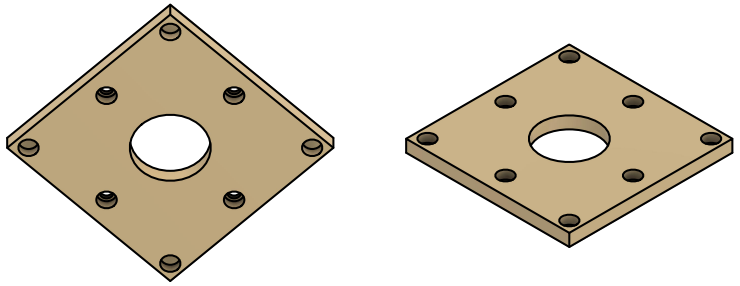

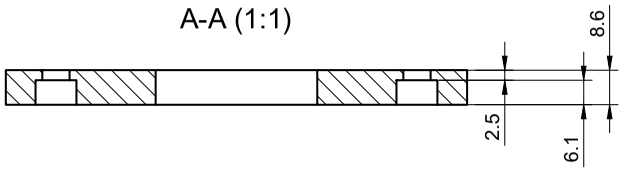

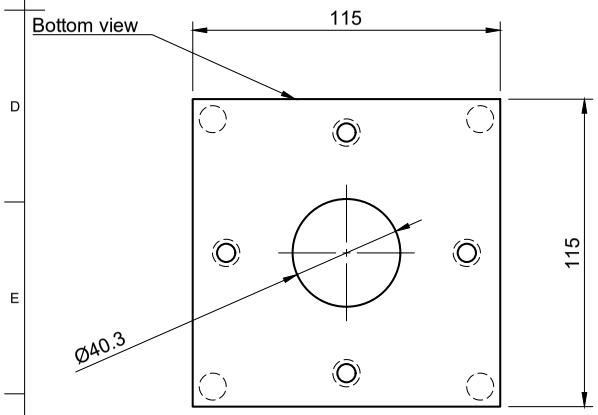

Unit: mm

Note:

- **3D Printer Manufacture**
- **PLA Material**
- **3D Printer Hole Shrink: -0.3**

E.g
Disgn:Ø40.3, Actual:Ø40.0

Dept.	Technical reference	Created by	Approved by
ISAPS		Ming-Hsiang Kuo 2022/4/12	
		Document type	Document status
		Title: Base Plate	DWG No.: PPL202111003_KMH
		Rev.	Date of issue / Sheet: 1/1

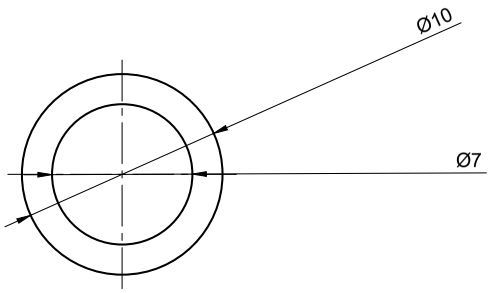

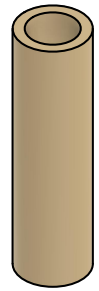

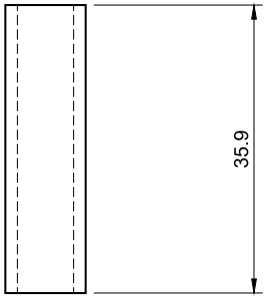

Unit: mm

Note:

- **3D Printer Manufacture**
- **PLA Material**
- **3D Printer Hole Shrink: -0.3**

E.g
Disgn:Ø7.0, Actual:Ø6.7

Dept.	Technical reference	Created by	Approved by
ISAPS		Ming-Hsiang Kuo 2022/4/12	
		Document type	Document status
		Title: Middle Column	DWG No.: PPL202111004_KMH
			Rev.: A / Date of issue / Sheet: 1/1

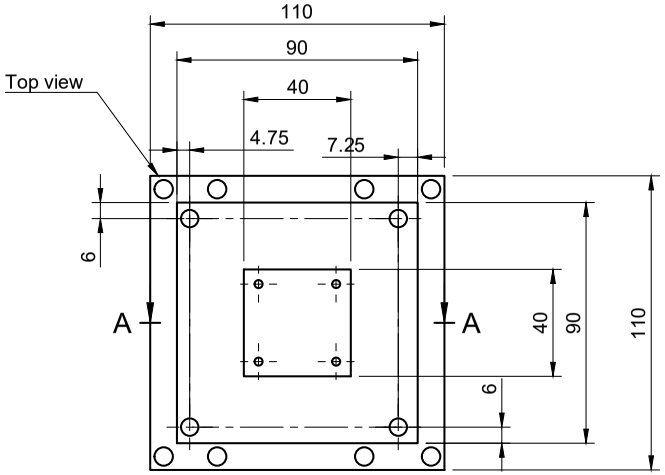

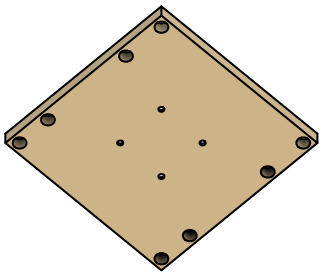

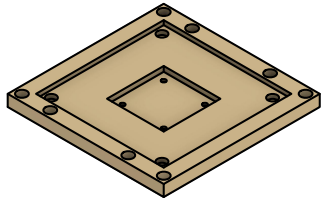

A-A (1:1)

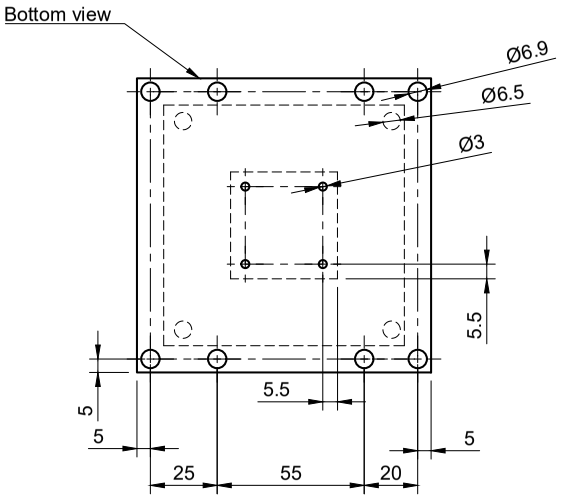

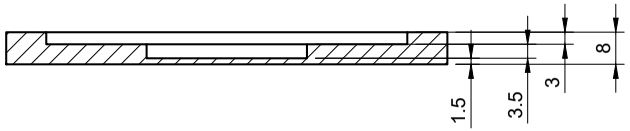

Unit: mm

Note:

- **3D Printer Manufacture**
- **PLA Material**
- **3D Printer Hole Shrink: -0.3**

E.g
Disgn:Ø6.9, Actual:Ø6.6

Dept.	Technical reference	Created by	Approved by
ISAPS		Ming-Hsiang Kuo 2022/4/12	
		Document type	Document status
		Title: Middle Plate	DWG No.: PPL202111005_KMH
		Rev.: A	Date of issue:	Sheet: 1/1

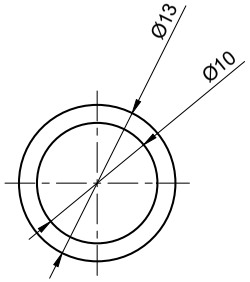

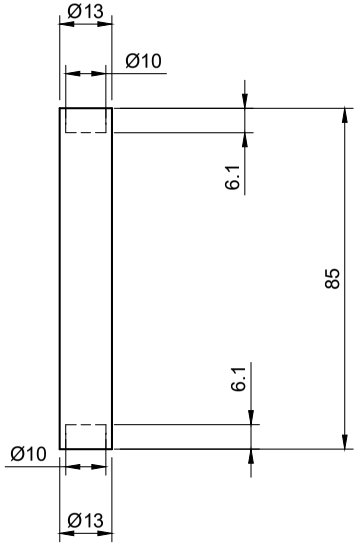

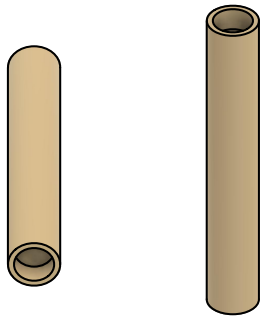

Unit: mm

Note:

- **3D Printer Manufacture**
- **PLA Material**
- **3D Printer Hole Shrink: -0.3**

E.g
Disgn:Ø10.0, Actual:Ø9.7

Dept.	Technical reference	Created by	Approved by
ISAPS		Ming-Hsiang Kuo 2022/4/13	
		Document type	Document status
		Title: Battery Column	DWG No.: PPL202111006_KMH
			Rev. / Date of issue / Sheet: 1/1

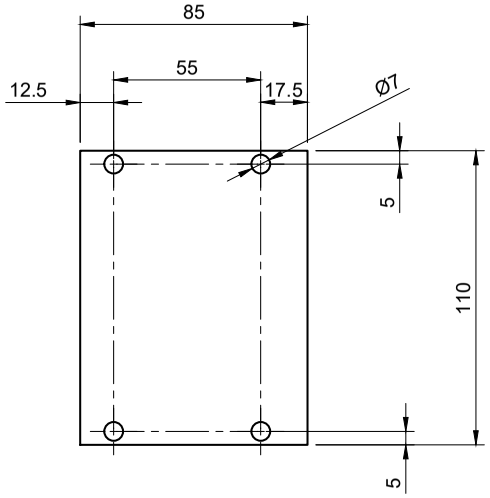

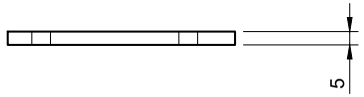

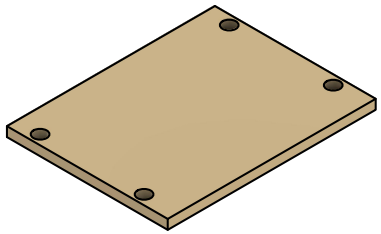

Unit: mm

Note:

- **3D Printer Manufacture**
- **PLA Material**
- **3D Printer Hole Shrink: -0.3**

E.g
Disgn:Ø7.0, Actual:Ø6.7

Dept.	Technical reference	Created by	Approved by
ISAPS		Ming-Hsiang Kuo 2022/4/13	
		Document type	Document status
		Title: Battery Plate	DWG No.: PPL202111007_KMH
			Rev.: A / Date of issue / Sheet: 1/1

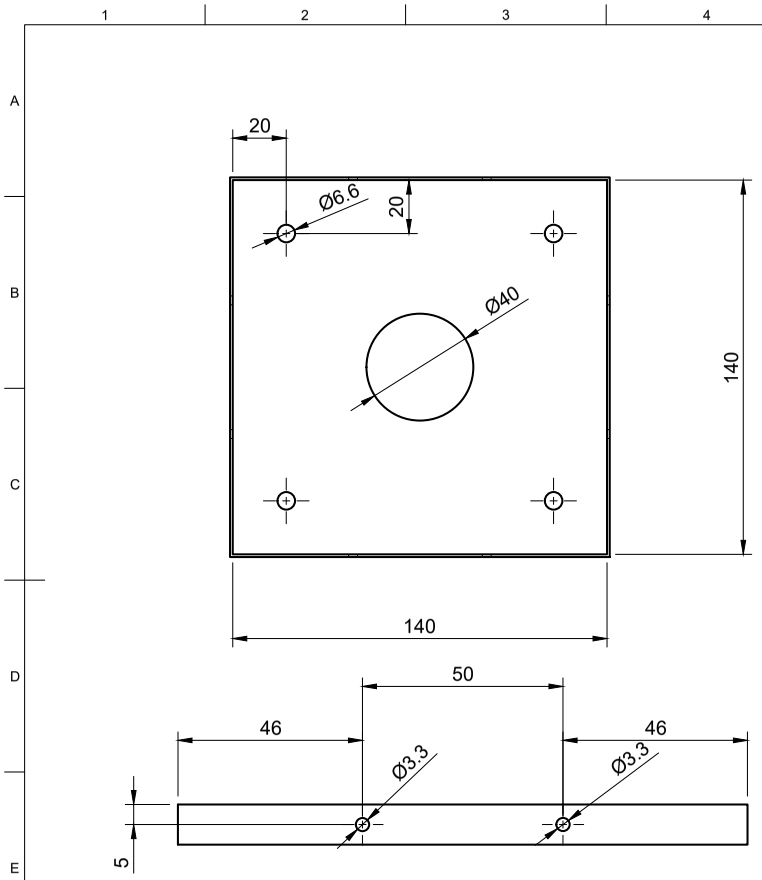

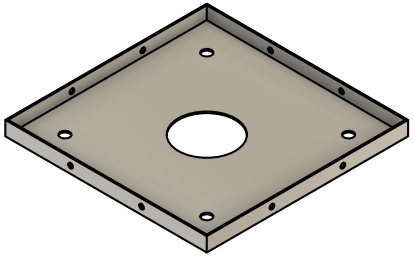

Dept.	Technical reference	Created by	Approved by
ISAPS		Ming-Hsiang Kuo 2021/11/19	
		Document type	Document status
		Title: Al Bottom	DWG No.: PPL202111008_KMH
			Rev.: A / Date of issue / Sheet: 1/1

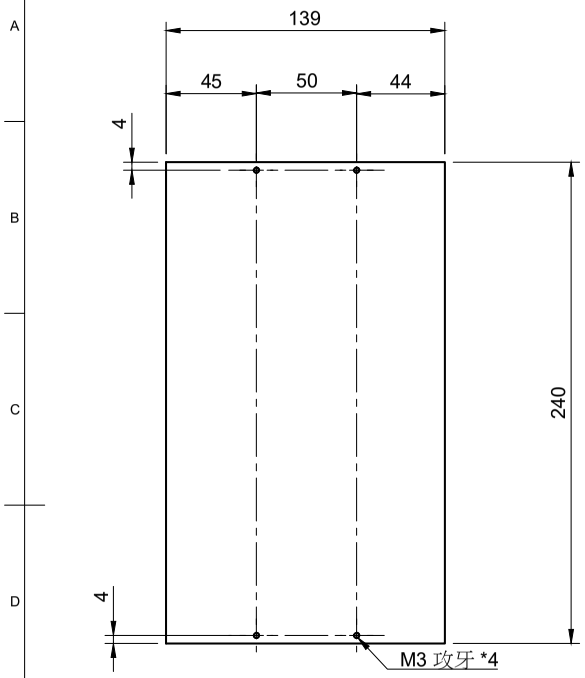

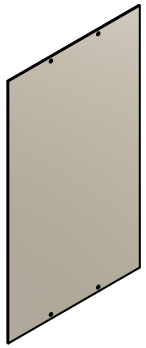

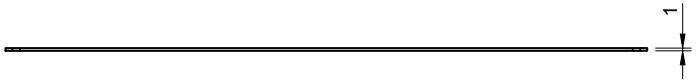

Dept.	Technical reference	Created by	Approved by
ISAPS		Ming-Hsiang Kuo 2022/4/13	
		Document type	Document status
		Title: Al side	DWG No.: PPI202111009_KMH
			Rev. / Date of issue / Sheet: 1/1

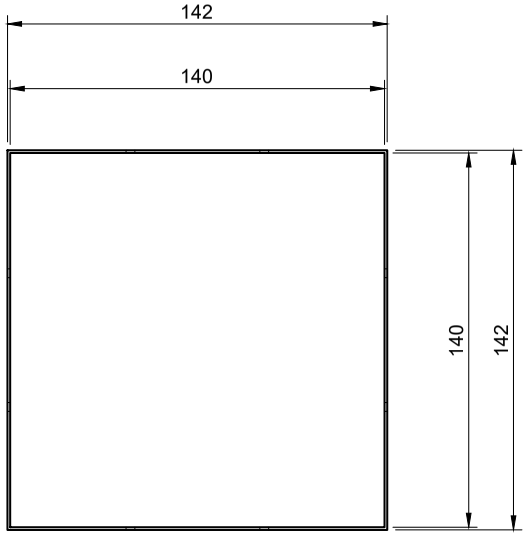

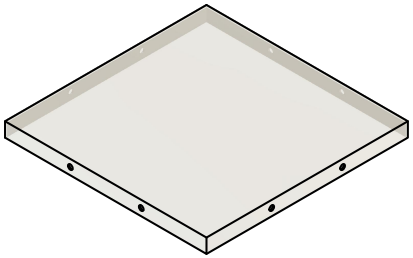

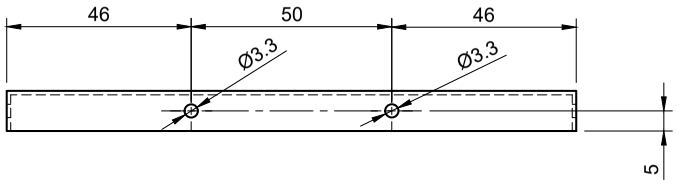

Dept. ISAPS	Technical reference	Created by Ming-Hsiang Kuo 2022/4/13	Approved by
		Document type	Document status
		Title Al top	DWG No. PPL202111010_KMH
			Rev. / Date of issue / Sheet 1/1